

1 Two promoters integrate multiple enhancer inputs to drive wild-type *knirps*  
2 expression in the *D. melanogaster* embryo

3 Lily Li, Rachel Waymack, Mario Elabd, Zeba Wunderlich

4 Department of Developmental and Cell Biology, University of California, Irvine, CA

5

6 Running Title: *Knirps* expression requires two promoters

7 Key words: promoter, enhancer, *knirps*, *Drosophila melanogaster*, enhancer–core-promoter  
8 specificity, polymerase initiation rate

9

10 Corresponding author:

11 Zeba Wunderlich

12 4107 Natural Sciences 2

13 Irvine, CA 92897

14 949-824-5959

15 [zeba@uci.edu](mailto:zeba@uci.edu)

16

17

18 **Abstract**

19 Proper development depends on precise spatiotemporal gene expression patterns. Most genes  
20 are regulated by multiple enhancers and often by multiple core promoters that generate similar  
21 transcripts. We hypothesize that these multiple promoters may be required either because  
22 enhancers prefer a specific promoter or because multiple promoters serve as a redundancy  
23 mechanism. To test these hypotheses, we studied the expression of the *knirps* locus in the early  
24 *Drosophila melanogaster* embryo, which is mediated by multiple enhancers and core promoters.  
25 We found that one of these promoters resembles a typical “sharp” developmental promoter, while  
26 the other resembles a “broad” promoter usually associated with housekeeping genes. Using  
27 synthetic reporter constructs, we found that some, but not all, enhancers in the locus show a  
28 preference for one promoter. By analyzing the dynamics of these reporters, we identified specific  
29 burst properties during the transcription process, namely burst size and frequency, that are most  
30 strongly tuned by the specific combination of promoter and enhancer. Using locus-sized reporters,  
31 we discovered that even enhancers that show no promoter preference in a synthetic setting have  
32 a preference in the locus context. Our results suggest that the presence of multiple promoters in  
33 a locus is both due to enhancer preference and a need for redundancy and that “broad” promoters  
34 with dispersed transcription start sites are common among developmental genes. Our results also  
35 imply that it can be difficult to extrapolate expression measurements from synthetic reporters to  
36 the locus context, where many variables shape a gene’s overall expression pattern.

37

38 **Introduction**

39 Diverse processes in biology, from early development to the maintenance of homeostasis, rely  
40 on the regulation of gene expression. Enhancers and promoters are the primary regions of the  
41 genome that encode these gene regulatory programs. Both enhancers and promoters are

42 characterized by clusters of sequence motifs that act as platforms for protein binding, allowing for  
43 the integration of a spectrum of signals in the cellular environment. The majority of studies that  
44 dissect enhancer or promoter function typically investigate each in isolation, which assumes that  
45 their function is largely modular. In practice, this means that we assume an enhancer drives  
46 generally the same pattern, regardless of promoter, and that promoter strength is independent of  
47 the interacting enhancer. However, there is evidence that there can be significant “interaction  
48 terms” between promoters and enhancers, with enhancer pattern shaped by promoter sequence,  
49 and promoter strength influenced by an enhancer (Gehrig et al., 2009; Hoppe et al., 2020; Qin et  
50 al., 2010).

51 Therefore, a key question is precisely how the sequences of an enhancer and a promoter  
52 combine to dictate overall expression output. Adding to the complexity of this question,  
53 developmental genes often have multiple enhancers, and many metazoan genes have alternative  
54 promoters (Brown et al., 2014; Landry, Mager, & Wilhelm, 2003; Schibler & Sierra, 1987;  
55 Schröder, Tautz, Seifert, & Jäckle, 1988). In a locus, multiple enhancers exist either because they  
56 drive distinct expression patterns or, in the case of seemingly redundant shadow enhancers,  
57 because they buffer noise in the system (Kvon, Waymack, Elabd, & Wunderlich, 2021). Though  
58 RAMPAGE data shows that >40% of developmentally expressed genes have more than one  
59 promoter (P. Batut, Dobin, Plessy, Carninci, & Gingeras, 2013), the role of multiple promoters has  
60 been relatively less explored. In some cases, alternative promoters drive distinct transcripts, but  
61 *hunchback* is a notable example of a gene with two highly conserved promoters that produce  
62 identical transcripts (Ling, Umezawa, Scott, & Small, 2019; Schröder et al., 1988).

63 This suggests there may be additional explanations for the prevalence of multiple  
64 promoters. One possibility is molecular compatibility—promoters can preferentially engage with  
65 different enhancers depending on the motif composition and proteins recruited to each (van  
66 Arensbergen, van Steensel, & Bussemaker, 2014; Wang, Hou, Quedenau, & Chen, 2016). For  
67 example, enhancers bound by either the transcription factors (TFs) Caudal or Dorsal tend to  
68 interact with Downstream Promoter Element (DPE)-containing promoters (Juven-Gershon, Hsu,  
69 & Kadonaga, 2008; Zehavi, Kuznetsov, Ovadia-Shochat, & Juven-Gershon, 2014) and Bicoid-  
70 dependent *hunchback* transcription seems to depend on the presence of a TATA box and Zelda  
71 site at one promoter (Ling et al., 2019). Another possibility is that having multiple promoters  
72 provides redundancy needed for robust gene expression, much like shadow enhancers.

73 To distinguish between these hypotheses, an ideal model is a gene with (1) multiple  
74 promoters that contain different promoter motifs and drive similar transcripts and with (2) multiple  
75 enhancers bound by different TFs. The *Drosophila* developmental gene *knirps* (*kni*) fits these  
76 criteria. It is a key developmental TF that acts in concert with other gap genes to direct anterior-  
77 posterior axis patterning of the early embryo. *Kni* has two core promoters that drive nearly identical  
78 transcripts (only differing by five amino acids at the N-terminus) and that are both used during the  
79 blastoderm stage (Figure 1A – C). Here, we define the core promoter as the region encompassing  
80 the transcription start site (TSS) and the 40bp upstream and downstream of the TSS (Vo Ngoc,  
81 Wang, Kassavetis, & Kadonaga, 2017). Also, like many early developmental genes, its precise  
82 pattern of expression in the blastoderm is coordinated by multiple enhancers (Figure 1A). These  
83 characteristics make the *kni* locus a good system in which to examine the roles of multiple  
84 promoters in a single gene locus.

85 We used several approaches to delineate the roles of these two promoters. To examine  
86 the molecular compatibility of different *kni* enhancer-promoter pairs in a controlled setting, we  
87 created reporter constructs of eight *kni* enhancer-promoter pairs driving expression of an MS2  
88 reporter. We found that some *kni* enhancers are able to interact with multiple promoters similarly,  
89 while others have a strong preference for one. By using the MS2 system to measure the  
90 transcription dynamics, we also determined the molecular events that lead to these preferences.  
91 Next, analysis of a *kni* locus reporter demonstrated that locus context can affect promoter-  
92 enhancer preferences and indicates that promoters both have different jobs and provide some  
93 amount of redundancy. Finally, we explored the role of different promoter motifs in specifying  
94 expression dynamics by using constructs with promoter mutations. Examining the *kni* locus has  
95 allowed us to (1) determine how transcription dynamics are impacted by molecular compatibility,  
96 (2) determine the roles of multiple promoters in a locus, and (3) probe how the motif content of  
97 promoters produces a particular expression output.  
98

## 99 Results

### 100 Selection of enhancers and promoter pairs tested

101 *knirps* has two conserved promoters that drive very similar transcripts (Figure 1A; Figure S1A and  
102 B). Most previous studies discuss the role of a single *kni* promoter (promoter 1), though in practice,  
103 many of the constructs used in these studies actually contained both promoters, since promoter  
104 2 is located in a *kni* intron (Bothma et al., 2015; El-Sherif & Levine, 2016; Pankratz et al., 1992;  
105 Pelegri & Lehmann, 1994). While more transcripts initiate from promoter 1 throughout most of  
106 development (Figure 1B), based on two different measures of transcript abundance, both  
107 promoters appear to be active during nuclear cycle 14, 2-3 hours after fertilization (Figure 1B and  
108 1C) (P. J. Batut & Gingeras, 2017; Lott et al., 2011). These two promoters are distinguished by  
109 their motif content and by their “shape” (Figure 1E). Promoter 1 is composed of multiple Initiator  
110 (Inr) motifs, each of which can specify a transcription start site. These Inr motifs enable promoter  
111 1 to drive transcription initiation in a 124 bp window, characteristic of a “broad” or “dispersed”  
112 promoter typically associated with housekeeping genes (Juven-Gershon, Hsu, Theisen, &  
113 Kadonaga, 2008; Sloutskin et al., 2015). There is a single DPE element in promoter 1; however,  
114 its significance is somewhat unclear, as it is only the canonical distance from a single, somewhat  
115 weak, Inr motif within the initiation window. Promoter 2 is composed of Inr, TATA Box and DPE  
116 motifs. This motif structure leads promoter 2 to initiate transcription in a 3 bp region, which is  
117 characteristic of the “sharp” or “focused” promoter shape typically associated with developmental  
118 genes (Figure S1C).

119 To select key early embryonic *kni* enhancers, we took into account the expression patterns  
120 driven by the enhancers and their overlap in the locus. We split the enhancers into three groups  
121 based on their expression patterns and selected one representative enhancer per group—  
122 enhancers driving a diffuse posterior stripe (*kni\_proximal\_minimal*), enhancers driving a sharp  
123 posterior stripe (*kni\_KD*, the “classic” *kni* posterior stripe enhancer), and enhancers driving the  
124 anterior band (*kni\_-5*) (Figure 1A). Among the enhancers driving a sharp posterior stripe, we  
125 decided to examine another enhancer, VT33935, in addition to *kni\_KD* (Pankratz et al., 1992).  
126 VT33935 was identified in a high-throughput screen for enhancer activity (Kvon et al., 2014) and  
127 has only minimal overlap with the *kni\_KD* enhancer but drives the same posterior stripe of  
128 expression. This suggests it may be an important contributor to *kni* regulation.

129 To determine the TF inputs to these enhancers, we scanned each enhancer using the  
130 motifs of TFs regulating early axis specification and calculated an overall binding capacity for  
131 each enhancer-TF pair (Figure 2A and S2). We found that kni\_KD and VT33935 seem to be  
132 regulated by similar TFs, which suggests that together they comprise one larger enhancer. Here,  
133 we studied them separately, as historically kni\_KD has been considered the canonical enhancer  
134 driving posterior stripe expression (Pankratz et al., 1992). Since kni\_KD, VT33935, and  
135 kni\_proximal\_minimal drive overlapping expression patterns, they can be considered a set of  
136 shadow enhancers. Despite their similar expression output, kni\_proximal\_minimal has different  
137 TF inputs than the other two, including different repressors and autoregulation by Kni itself (Perry,  
138 Boettiger, & Levine, 2011). kni\_-5 is the only enhancer that controls expression of a ventral,  
139 anterior band. Accordingly, this is the only enhancer of the four that has dorsal-ventral TF inputs  
140 (Dorsal and Twist) (Figure 2A) (Schroeder et al., 2004). In sum, analyses of the total binding  
141 capacity of these enhancers demonstrate that they are bound by different TFs (Figure 2A).

142 By using this set of endogenously interacting enhancers and promoters with varied motif  
143 content, we can elucidate the functional value of having multiple promoters. In particular, we can  
144 determine whether multiple promoters exist because different enhancers work with different  
145 promoters, or whether having multiple promoters provides necessary redundancy in the system,  
146 or some combination of the two.

147

#### 148 **Some enhancers tolerate promoters of different shapes and composition**

149 To characterize the inherent ability of promoters and enhancers to drive expression, without  
150 complicating factors like enhancer competition, promoter competition, or variable enhancer-  
151 promoter distances, we created a series of eight transgenic enhancer-promoter reporter lines.  
152 Each reporter contains one enhancer and one promoter directly adjacent to each other, followed  
153 by MS2 stem loops inserted in the 5' UTR of the *yellow* gene (Figure 1D, see Methods for details).  
154 These tagged transcripts are bound by MCP-GFP fusion proteins, yielding fluorescent puncta at  
155 the site of nascent transcription. The fluorescence intensity of each spot is proportional to the  
156 number of transcripts in production at a given moment (Garcia, Tikhonov, Lin, & Gregor, 2013).

157 When considering the expression output driven by these enhancer-promoter  
158 combinations, several outcomes are possible. One possible outcome is that one promoter is  
159 simply stronger than the other – consistently driving higher expression, regardless of which  
160 enhancer it is paired with. Another possibility is that each enhancer drives higher expression with  
161 one promoter than with the other, but this preferred promoter differs between enhancers. This  
162 would suggest that promoter motifs and shape affect their ability to successfully interact with  
163 enhancers with different bound TFs to drive expression. Lastly, it is possible that some enhancers  
164 drive similar expression with either promoter, this suggests that the particular set (and orientation)  
165 of the TFs recruited to those enhancers allow them to transcend the differences in promoter  
166 architecture.

167 When comparing the mean expression levels, we found that some enhancers (kni\_-5 and  
168 kni\_proximal\_minimal) have relatively mild preferences for one promoter over the other (Figure  
169 2B; two-sided *t*-test comparing kni\_-5-promoter1 vs. kni\_-5-promoter2,  $p = 0.12$  and  
170 kni\_proximal\_minimal-promoter1 vs. kni\_proximal\_minimal-promoter2  $p = 9.8 \times 10^{-5}$ ). Despite  
171 the significant differences between these enhancer-promoter constructs, the effect size is  
172 relatively small, with the largest difference in mean expression being 1.2-fold. This suggests that

173 the TFs recruited to these enhancers can interact with very different promoters more or less  
174 equally well. On the other hand, *kni\_KD* and *VT33935* respectively drive 2.9-fold and 3.2-fold  
175 higher expression with promoter 2 than promoter 1 at 62.5% embryo length ([Figure 2C](#); one-sided  
176 *t*-test  $p < 2.2 \times 10^{-16}$  for both). This suggests that the TFs recruited to *kni\_KD* and *VT33935*, which  
177 are similar, ([Figure 2A](#)) limit their ability to successfully drive expression with promoter 1, which  
178 is a dispersed promoter. Taken together, this implies a simple model of promoter strength is not  
179 sufficient to account for these results. Instead, it is the combination of the proteins recruited to  
180 both enhancers and promoters that set expression levels, with some enhancers interacting  
181 equally well with both promoters and others having a preference.

182 These differences in enhancer preference or lack thereof may be mediated by the  
183 particular TFs recruited to them and the motifs present in the promoters. Previous researchers  
184 have found that the developmental TFs, Caudal (Cad) and Dorsal (DI), tend to regulate genes  
185 with DPE motifs and drive lower expression when DPE has been eliminated (Juven-Gershon,  
186 Hsu, & Kadonaga, 2008; Zehavi et al., 2014). In addition, computational analysis of TF-promoter  
187 motif co-occurrence patterns indicates that Bcd shows a similar enrichment for DPE-containing  
188 promoters and a depletion for Inr- and TATA box-containing promoters when DPE is absent  
189 ([Figure S2](#)). A study also indicated that Bcd can work in conjunction with Zelda to activate a TATA  
190 Box-containing promoter, but this combination does not appear to be widely generalizable (Ling  
191 et al., 2019). In accordance with that, we find that all four *kni* enhancers, which bind Cad and Bcd,  
192 drive relatively high expression with the DPE-containing promoter 2. Interestingly, in the case of  
193 *kni\_-5* and *kni\_pm*, we find that they can also drive similarly high expression with the series of  
194 weak Inr sites that composes promoter 1. This indicates that while some factors mediating  
195 enhancer-promoter preference have been identified, there are additional factors we have yet to  
196 discover that are playing a role.

197 We also calculated the expression noise associated with each construct and plotted it  
198 against the expression output of each. Previous studies have suggested that TATA-containing  
199 promoters generally drive more noisy expression (Ramalingam, Natarajan, Johnston, & Zeitlinger,  
200 2021; Ravarani, Chalancon, Breker, de Groot, & Babu, 2016). Among our constructs, expression  
201 noise is generally inversely correlated with mean expression ([Figure 2C and 2D](#)), and the TATA-  
202 containing promoter 2 does not have uniformly higher noise than the TATA-less promoter 1.  
203 However, some constructs, notably those containing *kni\_-5*, have higher noise than others with  
204 similar output levels, suggesting that, in this case, promoters alone do not determine expression  
205 noise.

206

## 207 **Simple model of transcription and molecular basis of burst properties**

208 To unravel the molecular events that result in these expression differences, we consider our  
209 results in the context of the two-state model of transcription (Peccoud & Ycart, 1995; Tunnacliffe  
210 & Chubb, 2020). Here, the promoter is either (1) in the inactive state ("OFF"), in which RNA  
211 polymerase cannot initiate transcription or (2) in the active state ("ON"), in which it can ([Figure 3A](#)).  
212 The promoter transitions between these two states with rates  $k_{on}$  and  $k_{off}$ , with the transitions  
213 involving both the interaction of the enhancer and promoter and the assembly of the necessary  
214 transcriptional machinery. This interaction may be through direct enhancer-promoter looping or  
215 through the formation of a transcriptional hub, a nuclear region with a high concentration of TFs,  
216 co-factors, and RNA polymerase (Lim & Levine, 2021). For simplicity, we will use looping as a

217 shorthand to include both scenarios. In its active state, the promoter produces mRNA at rate  $r$ ,  
218 and given our ability to observe only nascent transcripts, the mRNA decay rate  $\mu$  denotes the  
219 diffusion of mRNA away from the gene locus.

220 We track these molecular events by analyzing the transcription dynamics driven by each  
221 reporter and quantifying several properties. Total expression is simply the integrated signal driven  
222 by each reporter. The burst duration is the period of active transcription, and is dependent on  $k_{off}$ ,  
223 the rate of dissociation of enhancer and promoter looping (Figure 3B). The burst size, or number  
224 of transcripts produced per burst, depends on the burst duration and the RNA Pol II initiation rate.  
225 (Short, aborted transcripts and paused PolII are not visible in MS2 measurements). The burst  
226 frequency, or the inverse of the time between two bursts, depends on both  $k_{on}$  and  $k_{off}$ . Previous  
227 work in the early embryo has shown burst duration (and thus  $k_{off}$ ) to be reasonably consistent  
228 regardless of enhancer and promoter (Waymack, Fletcher, Enciso, & Wunderlich, 2020; Yokoshi,  
229 Cambón, & Fukaya, 2021). Within this regime, burst frequency is mainly dependent on  $k_{on}$ . We  
230 used this model to characterize how the transcription output produced is affected by different  
231 combinations of the *kni* enhancers and promoters.

232

### 233 **Using GLMs to parse the role of enhancers, promoters, and their interactions**

234 To parse the role of enhancers, promoters, and their interactions more clearly in  
235 determining expression levels in these reporters, we built separate generalized linear models  
236 (GLMs) to describe each transcriptional property. We visually represented the model using a bar  
237 graph (Figure 4A) in which the contributions of enhancer, promoter, and their interactions are  
238 represented in bars of green, purple, and brown, respectively (Figure 4B). Since the relative  
239 differences in expression driven by different enhancer-promoter pairs are generally consistent  
240 across the AP axis, we used the expression levels at the location of maximum expression along  
241 the AP axis (22% and 63% for the anterior band and posterior stripe, respectively, Figure 2C).

242 If the molecular compatibility of the proteins recruited to the enhancer and promoter are  
243 important in determining a particular property, then we should find the interaction terms (in brown)  
244 to be sizeable in comparison with those of the enhancers (in green) and promoter (in purple). If  
245 not, the interaction terms will be relatively small. To develop an intuition for this formalism, we first  
246 built a GLM to describe total expression output. Using the GLM, we can see that enhancer,  
247 promoter, and interactions terms each play an important role in determining the expression output  
248 (Figure 4C), consistent with our qualitative interpretation above.

249 To determine which molecular events are modulated by molecular compatibility, we then  
250 applied this same GLM structure to each burst property. For example, molecular compatibility  
251 could increase the probability of enhancer-promoter loop formation, hence increasing the burst  
252 frequency. Alternatively, molecular compatibility could increase the rate at which RNA PolII  
253 initiates transcription, increasing burst size.

254

### 255 **Burst frequency and initiation rate are the primary determinants of expression levels**

256 We found that the differences in total expression output are primarily mediated through  
257 differences in burst size (Figure 4E) and burst frequency (Figure 4D). Burst duration is very  
258 consistent across all constructs (Figure 4F). While the enhancer, promoter, and interaction terms  
259 all have a significant impact on duration (multivariate ANOVA; enhancer:  $p = 4.4 \times 10^{-10}$ ; promoter:  
260  $p = 4.1 \times 10^{-5}$ ; interaction:  $p = 4.6 \times 10^{-5}$ ), the effect size is small, with the largest difference being

261 only 1.3-fold. Since burst size can be modulated by initiation rate and burst duration, and burst  
262 duration is relatively constant, this suggests that initiation rate and burst frequency are the primary  
263 dials used to tune transcription in these synthetic constructs.

264 Burst size is strongly dependent on both the enhancer and interaction terms; the  
265 interaction terms are a proxy for molecular compatibility. Of the variability in burst size explained  
266 by this model, enhancers and interaction terms account for 67.6% and 23.7% of the variance,  
267 respectively (Figure 4E). The differences in burst size were mainly achieved by tuning PolII  
268 initiation rate (Figure 4G). Conversely, burst frequency is dependent on promoter and enhancer  
269 identity, with negligible interaction terms (Figure 4D). Since burst frequency mainly depends on  
270 association rate ( $k_{on}$ ), this suggests that both enhancers and promoters play a large role in  
271 determining the likelihood of promoter activation, with molecular compatibility only minimally  
272 affecting this likelihood.

273 It is somewhat surprising that molecular compatibility plays only a small role in determining  
274  $k_{on}$ , since one might expect the interactions between the proteins recruited to promoters and  
275 enhancers would determine the likelihood of promoter-enhancer looping. This may be the result  
276 of the design of these constructs, with promoters and enhancer immediately adjacent to each  
277 other, and this may differ in a more natural context (see below). However, we do observe that  
278 molecular compatibility is important in determining the PolII initiation rate. This suggests that the  
279 TFs and cofactors recruited to each reporter may act synergistically to both recruit RNA PolII to  
280 the promoter and promote its successful initiation. In sum, these results indicate that not only do  
281 enhancer, promoter, and their molecular compatibility affect expression output, but they do so by  
282 tuning different burst properties in this synthetic setting.

283

#### 284 **Despite promoter 2's compatibility with kni\_-5, promoter 1 primarily drives anterior 285 expression in the locus context**

286 The constructs measured thus far only contain a single enhancer and promoter, and therefore  
287 measure the inherent ability of a promoter and enhancer to drive expression. However, in the  
288 native locus, other complications like differing enhancer-promoter distances, enhancer  
289 competition, or promoter competition may impact expression output. To measure the effect of  
290 these complicating factors, we cloned the entire *kni* locus into a reporter construct and measured  
291 the expression patterns and dynamics of the wildtype locus reporter (wt) and reporters with either  
292 promoter 1 or 2 knocked out ( $\Delta p1$  and  $\Delta p2$ ) (Figure 5A). Due to the large number of Inr motifs, we  
293 made the  $\Delta p1$  construct by replacing promoter 1 with a piece of lambda phage DNA. To make the  
294  $\Delta p2$  construct, we inactivated the TATA, Inr, and DPE motifs by making several mutations (see  
295 Methods for additional details).

296 In the anterior, the *kni\_-5* enhancer is solely responsible for driving expression. Therefore,  
297 by comparing the expression output from the wildtype locus reporter and the *kni\_-5*-promoter  
298 reporters in the anterior, we can measure the effect of the locus context, i.e. multiple promoters,  
299 differing promoter-enhancer distance, or other DNA sequence features. If the *kni\_-5*-promoter  
300 reporters capture their ability to drive expression in the locus context, we would expect the locus  
301 reporter to drive expression equal to the sum of the *kni\_-5*-p1 and *kni\_-5*-p2 reporters. In contrast  
302 to this expectation, in the anterior band, the locus reporter drives a much lower level of expression  
303 than the sum of the two *kni\_-5* reporters (Figure 5B, dark purple vs black bar). In fact, the level is

304 similar to the expression output of *kni*\_5 paired with either individual promoter, suggesting that  
305 *kni*\_5's expression output is altered by the locus context.

306 The observed sub-additive behavior may arise in several ways. It may be that promoter  
307 competition similarly reduces the expression output of both p1 and p2 in the anterior. In this case,  
308 knocking out either promoter would produce wildtype levels of expression, as competition would  
309 be eliminated. Alternatively, the ability to drive expression in the locus context could be uneven  
310 between the promoters. If this is the case, we would expect the promoter knockouts to have  
311 different effects on expression.

312 Consistent with the second scenario, we find that when promoter 2 is eliminated in the *kni*  
313 locus construct, the expression in the anterior remains essentially the same (two-sided *t*-test  
314 comparing mean expression levels of wt vs.  $\Delta p_2$ ,  $p = 0.62$ ), while a promoter 1 knockout has a  
315 significant impact on expression levels (one-sided *t*-test comparing mean expression levels of wt  
316 vs.  $\Delta p_1$ ,  $p < 2.2 \times 10^{-16}$ , [Figure 5B](#)). Thus, promoter 1 is sufficient to produce wildtype expression  
317 levels and patterns in the locus. The noise and the burst properties of the WT *kni* locus construct  
318 and the promoter 2 knockout are also nearly identical to the wildtype locus, further supporting the  
319 claim of promoter 1 sufficiency in the anterior ([Figure 5C – G](#)). Notably, even in a locus that  
320 contains promoters with and without a canonically placed DPE element (promoter 2 vs promoter  
321 1), a Cad- and DI-binding enhancer like *kni*\_5, can still primarily rely on the DPE-less promoter  
322 1 to drive transcription.

323 When promoter 1 is eliminated from the locus, expression is cut to about one third of that  
324 of the wildtype locus construct, which is also lower than the expression output of the *kni*\_5-p2  
325 construct. Thus, unlike promoter 1, promoter 2 loses its ability to drive wildtype levels of  
326 expression in the context of the locus. As promoter 2 is ~650bp upstream of promoter 1, this extra  
327 distance between *kni*\_5 and promoter 2 may be sufficient to reduce promoter 2's ability to drive  
328 expression. Alternatively, other features of the *kni* locus, such as the binding of other proteins or  
329 topological constraints, may interfere with the ability of the *kni*\_5 enhancer to effectively interact  
330 with promoter 2. The drop in expression is mediated by a tuning down of all burst properties  
331 ([Figure 5D – G](#)). In sum, the *kni*\_5 enhancer preferentially drives expression via promoter 1 in  
332 the locus, even though enhancer-promoter constructs indicate that it is equally capable of driving  
333 expression with promoter 2. When promoter 1 is absent from the locus, promoter 2 is able to drive  
334 a smaller amount of expression, suggesting that it can serve as a backup, albeit an imperfect one.  
335

### 336 **In the posterior, both promoters are required for wildtype expression levels**

337 The posterior stripe is controlled by three enhancers, with *kni*\_proximal\_minimal producing similar  
338 levels of transcription with either promoter, and the other two enhancers strongly preferring  
339 promoter 2 and driving lower expression overall ([Figure 2B](#)). Therefore, when considering the  
340 posterior stripe, the expression output of the locus reporter may differ from the individual  
341 enhancer-reporter constructs due to promoter competition, enhancer competition, different  
342 promoter-enhancer distances, or other DNA features. By comparing the sum of the six relevant  
343 enhancer-promoter reporters to the output of the locus reporter, we can see that the locus  
344 construct drives considerably lower expression levels than the additive prediction ([Figure 5B, dark](#)  
345 [purple vs black bar](#)). In fact, the locus reporter output levels are similar to the sum of the enhancer-  
346 promoter 2 reporters, suggesting that promoter 2 could be solely responsible for expression in  
347 the posterior, despite *kni*\_proximal\_minimal's ability to effectively drive expression with promoter

348 1. If promoter 2 is sufficient for posterior stripe expression, we would predict that the promoter 1  
349 knockout would have a relatively small effect, while a promoter 2 knockout would greatly decrease  
350 expression in the posterior.

351 In contrast to this expectation, both promoter 1 and promoter 2 knockouts have a sizable  
352 effect on expression output, indicating that both are required for wildtype expression levels in the  
353 posterior (Figure 5B, light gray and gray bars). Specifically, knocking out promoter 2 severely  
354 reduces expression in the posterior stripe, producing about half the expression of the summed  
355 outputs of the enhancer-promoter1 constructs (Figure 5B, light gray vs light purple bars).  
356 Knocking out promoter 1 also reduces expression in the posterior stripe but not as severely as  
357 knocking out promoter 2 (Figure 5B, gray vs light gray bars). The promoter 1 knockout generates  
358 about half the expression of the summed expression output of the enhancer-promoter2 constructs  
359 (Figure 5B, gray vs purple bars). In both cases, the results indicate that the differences in locus  
360 context cause the enhancers to act sub-additively, even when only one promoter is present.

361 The promoter knockouts also allow us to examine how they tune expression output.  
362 Knocking out either promoter impacts burst size (and thus initiation rate) and burst frequency,  
363 though knocking out promoter 2 has a more severe impact (Figure 5D, 5E and 5G). These results  
364 show that, in the posterior, both promoters are required to produce WT expression levels when  
365 considered in the endogenous locus setting (Figure 5B, light and dark gray vs black bars). This is  
366 despite the fact that enhancer-promoter reporters indicate that, in the absence of competition,  
367 promoter 2 alone would suffice (Figure 5B, purple vs black bars).

368  
369 **PoIII initiation rate is a key burst property that is tuned by promoter motif**  
370 Studying these enhancers and promoters in the locus context demonstrated that distance and  
371 competition affect a promoter's ability to drive expression, but now we narrow our focus to  
372 promoter 2's remarkable compatibility with enhancers that bind very different sets of TFs. To  
373 dissect how its promoter motifs enable promoter 2 to be so broadly compatible, we again made  
374 enhancer-promoter reporter lines in which one enhancer and one promoter are directly adjacent  
375 to each other, but this time the promoter is a mutated promoter 2 in which the TATA Box and DPE  
376 motifs have been eliminated (Figure 6A, see Methods for details). This allows us to determine  
377 whether a single, strong Inr site (mutated promoter 2) can perform similarly to a series of weak  
378 Inr sites (promoter 1) and to clarify the role of TATA Box and DPE motifs in tuning burst properties.

379 Promoter 2 is characterized by two TATA Boxes, an Inr motif, and a DPE motif. Previously,  
380 much research has focused on comparing TATA-dependent with DPE-dependent promoters;  
381 however, many promoters contain both. Here, we consider how the presence of both may impact  
382 transcription. We know that each of these motifs recruits subunits of TFIID, with TATA Box  
383 recruiting TBP or TRF1 (Hansen, Takada, Jacobson, Lis, & Tjian, 1997; Holmes & Tjian, 2000;  
384 Kim, Nikolov, & Burley, 1993), Inr recruiting TAF1 and 2 (Chalkley & Verrijzer, 1999; Wu et al.,  
385 2001), and DPE recruiting TAF6 and 9 (Shao et al., 2005), as well as other co-factors like CK2  
386 and Mot1 (Hsu et al., 2008; Lewis, Sims, Lane, & Reinberg, 2005). Strict spacing between TATA-  
387 Inr and Inr-DPE both facilitate assembly of all these factors and others into a pre-initiation complex  
388 (Burke & Kadonaga, 1996; Emami, Jain, & Smale, 1997). It is likely that a promoter with all three  
389 motifs will behave similarly, with the addition of each motif further tuning the composition,  
390 configuration, or flexibility of the transcriptional complex. Given this, elimination of the TATA Box  
391 and DPE motifs may weaken the promoter severely through loss of cooperative interactions,

392 especially for *kni\_KD* and *VT33935*, which are significantly more compatible with promoter 2 than  
393 promoter 1. Alternatively, the single strong *Inr* site may be sufficient to recruit the necessary  
394 transcription machinery, especially in the case of *kni\_-5* and *kni\_proximal\_minimal*, which work  
395 well with the series of weak *Inr* sites that composes promoter 1.

396 When compared to promoter 1, we see that promoter 1-compatible enhancers (*kni\_-5* and  
397 *kni\_proximal\_minimal*) drive lower expression with a single *Inr* than with a series of weak *Inr* sites  
398 ([Figure 6B, light purple bars](#)). In contrast, enhancers less compatible with promoter 1 (*kni\_KD*  
399 and *VT33935*) drive higher expression with a single *Inr* site than promoter 1 even without the  
400 TATA Box and DPE sites ([Figure 6B, light purple bars](#)), suggesting that the strong *Inr* is the key  
401 to better expression output with these enhancers. For all enhancers, the resulting expression  
402 change appears to be mediated mainly through a decrease in burst size due to a reduction in  
403 initiation rates ([Figure 6D – F](#)).

404 Given that all four enhancers are compatible with promoter 2, and promoter 2 appears to  
405 achieve higher expression by tuning PolII initiation rates, we posit that TATA Box and DPE are  
406 what help promoter 2 drive high initiation rates. When comparing  $p2\Delta TATA\Delta DPE$  with promoter  
407 2, we see that all enhancers produce lower expression ([Figure 6B, dark purple bars](#)), and this is  
408 mediated mainly through tuning burst size ([Figure 6D](#)) and, for some enhancers, also burst  
409 frequency ([Figure 6C](#)). Notably, burst size (and thus polymerase initiation rate), which were most  
410 dependent on molecular compatibility, are affected the most by the elimination of the TATA Box  
411 and DPE motifs ([Figure 6D and 6E](#)), indicating that molecular compatibility plays an important  
412 role mediating high expression output. Interestingly, even in the absence of the TATA Box and  
413 DPE motifs, the one strong *Inr* site is sufficient to produce higher expression with the enhancers  
414 less compatible with promoter 1 (*kni\_KD* and *VT33935*), and this increased expression is also  
415 mediated by higher polymerase initiation rates ([Figure 6B and 6F, light purple bars](#)). In conclusion,  
416 enhancers seem to fall into classes, which behave in similar ways with particular promoters, and  
417 the molecular compatibility that appears to tune PolII initiation rates seems to be mediated by the  
418 promoter motifs present in an enhancer-specific manner.

419

## 420 Discussion

421 We dissected the *kni* gene locus as a case study of the role of multiple promoters in controlling a  
422 single gene's transcription dynamics. Synthetic enhancer-promoter reporters allowed us to  
423 measure the ability of *kni* enhancer-promoter pairs to drive expression in the absence of  
424 complicating factors like promoter or enhancer competition. Using these reporters, we found that  
425 some promoters are broadly compatible with many enhancers, whereas others only drive high  
426 levels of expression with some enhancers. A detailed analysis of the transcription dynamics of  
427 these reporters indicates that the molecular compatibility of the proteins recruited to the enhancer  
428 and promoter tune expression levels by altering the initiation rate of transcriptional bursts.

429 In the context of the whole locus, we found that some enhancer-promoter pairs drive lower  
430 expression than their corresponding synthetic reporters, due to the effects of promoter and  
431 enhancer competition, distance, or other factors. In fact, while the synthetic reporters indicate that  
432 both promoters can drive similarly high levels of expression in the anterior, in the locus, promoter  
433 1 drives most of the expression, with promoter 2 supporting some low levels of expression in the  
434 absence of promoter 1. In the posterior, both promoters appear to be necessary to achieve  
435 wildtype levels of expression with enhancer competition leading to sub-additive expression. By

436 mutating promoter motifs in the synthetic enhancer-reporter constructs, we found that the effects  
437 of promoter motif mutations fall into two different classes, depending on the enhancer that is  
438 paired with the promoter. This suggests that there may be several discrete ways that a promoter  
439 can be activated by an enhancer, depending on the proteins recruited to each. Returning to our  
440 original hypotheses to explain the presence of two promoters in a single locus, we find that both  
441 differing enhancer-promoter preferences and a need for expression robustness in the face of  
442 promoter mutation may play a role.

443 Our work has highlighted the importance of both of *kni*'s promoters. Previous studies have  
444 almost exclusively focused on *kni*'s promoter 1 (Pankratz et al., 1992; Pelegri & Lehmann, 1994),  
445 which unexpectedly looks like a typical housekeeping gene promoter, with a dispersed shape and  
446 series of weak Inr sites (Vo Ngoc et al., 2017). It is *kni*'s promoter 2, with its focused site of  
447 initiation and composition of TATA Box, Inr, and DPE motifs, that looks like a canonical  
448 developmental promoter (Vo Ngoc et al., 2017). Interestingly, despite only discussing promoter  
449 1, in practice, studies interrogating the behavior of multiple *kni* enhancers often included both  
450 promoters, as promoter 2 is found in a *kni* intron (Bothma et al., 2015; El-Sherif & Levine, 2016).  
451 Our analysis clearly demonstrates both promoters' vital role in normal *kni* expression.

452 With these observations in mind, we wanted to determine the prevalence of a two-  
453 promoter structure, with one broad and one sharp. To do so, we used the RAMPAGE data set,  
454 which includes a genome-wide survey of promoter usage during the 24 hours of *Drosophila*  
455 embryonic development (P. J. Batut & Gingeras, 2017) and cross-referenced these promoters  
456 with those in the Eukaryotic Promoter Database, which is a collection of experimentally validated  
457 promoters (Dreos, Ambrosini, Groux, Cavin Périer, & Bucher, 2016). We found that 13% of  
458 embryonically expressed genes have at least two promoters. When we considered the two most  
459 commonly used promoters, there is a clear trend of a broader primary (most used) promoter  
460 (median = 91bp) and a sharper secondary promoter (median = 42bp) (Figure S1C). This trend is  
461 still present if the genes are split into developmental and housekeeping genes, with  
462 developmental promoters (median = 43bp) generally more focused than housekeeping promoters  
463 (median = 90bp), as expected (Figure S1D and E). Among the primary promoters of  
464 developmental genes, 58% consist of a series of weak Inr sites, much like *kni* promoter 1. This  
465 suggests that this promoter shape and motif content in developmental promoters may be more  
466 common than previously expected and should be explored.

467 There is growing evidence that promoter motifs play a role in modulating different aspects  
468 of transcription dynamics. However, the role of each motif can vary from one locus to the next. In  
469 the "TATA-only" *Drosophila snail* promoter, the TATA Box affects burst size by tuning burst  
470 duration (Pimmett et al., 2021). In the mouse PD1 proximal promoter, which consists of a CAAT  
471 Box, TATA Box, Sp1, and Inr motif, the TATA box may tune burst size and frequency (Hendy,  
472 Campbell, Weissman, Larson, & Singer, 2017). A study of a synthetic *Drosophila* core promoter  
473 and the *ftz* promoter found that the TATA box tunes burst size by modulating burst amplitude and  
474 that Inr, MTE, and DPE tune burst frequency (Yokoshi et al., 2021). TATA Box also appears to  
475 be associated with increased expression noise, as TATA-containing promoters tend to drive  
476 larger, but less frequent transcriptional bursts (Ramalingam et al., 2021). In contrast to TATA Box,  
477 Inr appears to be associated with promoter pausing, e.g. by adding a paused promoter state in  
478 the Inr-containing *Drosophila Kr* and *llp4* promoters (Pimmett et al., 2021). In fact, a Pol II ChIP-

479 seq study indicates that paused developmental genes appear to be enriched for GAGA, Inr, DPE,  
480 and PB motifs (Ramalingam et al., 2021).

481 Similarly, the TFs bound at enhancers can affect transcription dynamics in diverse ways.  
482 Exploration of the role of TFs in modulating burst properties has indicated that BMP and Notch  
483 can tune burst frequency and duration, respectively (Falo-Sanjuan, Lammers, Garcia, & Bray,  
484 2019; Hoppe et al., 2020; Lee, Shin, & Kimble, 2019). Work that considers both the promoters  
485 and enhancer simultaneously have come to differing conclusions. Work in human Jurkat cells,  
486 wherein 8000 genomic loci were integrated with one of three promoters, showed that burst  
487 frequency is modulated at weakly expressed loci and burst size modulated at strongly expressed  
488 loci (Dar et al., 2012). Work in *Drosophila* embryos and in mouse fibroblasts and stem cells  
489 suggest that stronger enhancers produce more bursts, and promoters tune burst size (Fukaya,  
490 Lim, & Levine, 2016; Larsson et al., 2019). On the whole, this work indicates that promoter motifs  
491 and the TFs binding enhancers can act to tune burst properties in a myriad of ways. Given the  
492 wide range of possibilities, it is likely that setting, i.e. the combination of promoter motifs and the  
493 interacting enhancers, is particularly important in determining the resulting transcription dynamics.

494 Our work supports this notion. Notably, eliminating the TATA Box and DPE from promoter  
495 2 seems to reinforce the idea that we have two classes of enhancers that behave in distinct ways  
496 with these promoters due to the different TFs bound at these enhancers. We find that polymerase  
497 initiation rate is a key property tuned by the molecular compatibility of the proteins recruited to the  
498 enhancer and promoter. Our observation is in contrast to previous studies in which PolII initiation  
499 rate seems constant despite swapping two promoters with different motif content or altering BMP  
500 levels or the strength of TF's activation domains (Hoppe et al., 2020; Senecal et al., 2014) and is  
501 tightly constrained for gap genes (Zoller, Little, & Gregor, 2018). We suggest that the differences  
502 we see in our work, where initiation rate depends on molecular compatibility, versus other work,  
503 where initiation rate is controlled by other factors, again reinforces the idea that the role of any  
504 particular promoter motif or TF binding site can be highly context dependent.

505 Together, ours and previous work demonstrate that deriving a general set of rules to  
506 predict transcription dynamics from sequence is a challenge because the space of promoter motif  
507 content and enhancer TF binding site arrangements is enormous. The proteins recruited to both  
508 promoters and enhancers can combine to make transcriptional complexes with different  
509 constituent proteins, post-translational modifications, and conformations, which may even vary as  
510 a function of time. Due to the vast possibility space and context-dependent rules, we have likely  
511 only scratched the surface of how promoter motifs or enhancers can modulate burst properties,  
512 suggesting a field rich for future investigation.

513

514 **Acknowledgements**

515 The authors wish to thank Leonila Lagunes, Srikanth Chandrasekaran, and all the Wunderlich lab  
516 members for helpful comments on the manuscript and Ali Mortazavi, Kyoko Yokomori, Kevin  
517 Thornton, and Rahul Warrior for useful discussion on the project. The authors thank Flo Ramirez  
518 for data analysis that inspired some of this work.

519

520 **Funding**

521 This work is supported by NIH-NICHD R00 HD073191 and NIH-NICHD R01 HD095246 (to ZW)  
522 and the US DoE P200A120207 and NIH-NIBIB T32 EB009418 (to LL).

523

524 **Conflicts of Interest**

525 None to report.

526

527 **Materials and Methods**

528 **Datasets used in this study**

529 The experimentally validated promoters and their experimentally determined transcription start  
530 sites (TSSs) were obtained from the Eukaryotic Promoter Database (EPD) New (Dreos et al.,  
531 2016). They were cross-referenced with the RNA Annotation and Mapping of Promoters for  
532 Analysis of Gene Expression (RAMPAGE) data obtained from five species of *Drosophila* (P. J.  
533 Batut & Gingeras, 2017) to form a high-confidence set of promoters for which promoter usage  
534 during development could be evaluated. Single embryo RNA-seq obtained by Lott, et al. was  
535 indexed (with a  $k$  of 17 for an average mapping rate of 96%) and quantified using Salmon  
536 v0.12.01. The resulting transcript-specific data was used to further resolve *kni* promoter usage  
537 during nuclear cycle 14 (Lott et al., 2011; Patro, Duggal, Love, Irizarry, & Kingsford, 2017).  
538 Housekeeping genes were defined as in Corrales, et al. where genes were defined as  
539 housekeeping if their expression exceeded the 40<sup>th</sup> percentile of expression in each of 30 time  
540 points and conditions using RNA-seq data collected by modEncode (Corrales et al., 2017) and a  
541 list of these can be found in the Supplementary Materials ([File S1](#)).

542 To study TF-promoter motif co-occurrence, we collected a total of ~1000 enhancer-gene  
543 pairs expressed during development in *Drosophila*. The majority were identified by traditional  
544 enhancer trapping (REDfly & CRM Activity Database 2, or CAD2) and consist of non-redundant  
545 experimentally characterized enhancers (Bonn et al., 2012; Halfon, Gallo, & Bergman, 2008).  
546 About 15% were identified through functional characterization of ~7000 enhancer candidates  
547 using high throughput *in situ* hybridization (Vienna Tile, or VT); these VT enhancers have been  
548 limited to those expressed during stages 4-6. The remaining 1% of enhancer-gene pairs have  
549 been identified through 4C-seq (Ghavi-Helm et al., 2014) and are active 3-4 hours after egg laying  
550 (stages 6-7). A list of these enhancer-promoter pairs and their coordinates can be found in the  
551 Supplementary Materials ([File S2](#)).

552

553 **Motif prediction in promoters and enhancers**

554 For enhancers, TF binding site prediction was performed using Patser (Hertz & Stormo, 1999)  
555 with position weight matrices (PWMs) from the FlyFactor Survey (Zhu et al., 2011) and a GC  
556 content of 0.406. Each element in the PWM was adjusted with a pseudocount relative to the

557 intergenic frequency of the corresponding base totaling 0.01. For TFs that had multiple PWMs  
558 available, PWMs built from the largest number of aligned sequences were chosen; that of Stat92E  
559 was taken from an older version of the FlyFactor Survey. For promoters, the transcription start  
560 clusters (TSCs) (P. J. Batut & Gingeras, 2017) and the adjoining  $\pm 40$ bp were scanned for Inr,  
561 TATA Box, DPE, MTE, and TCT motifs using ElemeNT and the PWMs from (Sloutskin et al.,  
562 2015).

563

#### 564 **Evaluation of total binding capacity of enhancers**

565 Total binding capacity is a measure of the cumulative ability of an enhancer to bind a TF, and  
566 thus it takes into account the binding affinity of every  $w$ -mer in the enhancer for a TF binding site  
567 of length  $w$  (Wunderlich et al., 2012). To calculate the total binding capacity, we start by  
568 computationally scoring each possible site in the enhancer for the motifs of TFs regulating early  
569 axis specification. Taking the exponential of the score, normalizing this exponential by the  
570 enhancer length  $l$ , and summing these values gives us an overall binding capacity for each  
571 enhancer and TF combination, which is roughly equal to the sum of the probabilities that a TF is  
572 bound to each potential site in the enhancer.

573 Hence, we use the following formula

$$574 c(s, z) = \sum_{i=1}^{l-w+1} \frac{e^{\sum_{j=1}^w \ln \frac{p_j(b(j))}{q(b(j))}}}{l}$$

575 to calculate the total binding capacity  $c$  of a given sequence  $s$  for a given TF  $z$  (Wunderlich et al.,  
576 2012). Here,  $l$  is the length of the sequence being considered,  $w$  is the width of the PWM of the  
577 TF,  $b(i)$  is the base at position  $i$  of the sequence,  $p_j(b)$  is the frequency of seeing base  $b$  at  
578 position  $j$  of the PWM, and  $q(b)$  is the background frequency of base  $b$ . Note that  $\sum_{j=1}^w \ln \frac{p_j(b(j))}{q(b(j))}$   
579 is equivalent to the score given to the  $w$ -mer at position  $i$  in the sequence calculated using Patser,  
580 as described above (Hertz & Stormo, 1999).

581

#### 582 **Selection of enhancers to study**

583 *knirps* enhancers expressed in the blastoderm were identified using REDfly (Halfon et al., 2008),  
584 and the shortest, non-overlapping subset of enhancers was obtained using  
585 SelectSmallestFeature.py available at the Halfon Lab GitHub  
586 (<https://github.com/HalfonLab/UtilityPrograms>). The enhancers in this subset were categorized by  
587 the expression patterns they drove, and a representative enhancer was picked from each of these  
588 categories.

589

#### 590 **Generation of transgenic reporter fly lines**

591 As described in Fukaya, et al., the four *kni* enhancers were each cloned into the pBphi vector,  
592 directly upstream of *kni* promoter 1, 2 or  $2\Delta$ TATA $\Delta$ DPE; 24 MS2 repeats; and a *yellow* reporter  
593 gene (Fukaya et al., 2016). Similarly, the *kni* locus and its promoter knockouts ( $\Delta$ p1 and  $\Delta$ p2)  
594 were each cloned into the pBphi vector, directly upstream of 24 MS2 repeats and a *yellow* reporter  
595 gene by Applied Biological Materials (Richmond, BC, Canada). We defined *kni*\_5 as  
596 *chr3L*:20699503-20700905(–), *kni*\_proximal\_minimal as *chr3L*:20694587-20695245(–), *kni*\_KD  
597 as *chr3L*:20696543- 20697412(–), *VT33935* as *chr3L*:20697271-20699384(–), promoter 1 as

598 chr3L:20695324-20695479(–), promoter 2 as chr3L:20694506-20694631(–), and the *kni* locus as  
599 chr3L:20693955-20701078(–), using the *Drosophila melanogaster* dm6 release coordinates.  
600 Promoter motif knockouts (for p2ΔTATAΔDPE and locus Δp2) involved making the minimal  
601 number of mutations that would both inactivate the motif and introduce the fewest new motifs or  
602 TF binding sites (TATA: TATATATATC > TAGATGTATC, Inr: TCAGTT > TCGGTT, and DPE:  
603 AGATCA > ATACCA). The locus Δp1 construct involved replacing promoter 1 with a region of the  
604 lambda genome predicted to have the minimal number of relevant TF binding sites. The precise  
605 sequences for each reporter construct are given in a series of GenBank files included in the  
606 Supplementary Materials (File S3 – 18).

607 Using phiC31-mediated integration, each reporter construct was integrated into the same  
608 site on chr2L by injection into yw; PBac{y[+]-attP-3B}VK00002 (BDRC stock #9723) embryos by  
609 BestGene Inc (Chino Hills, CA). To visualize MS2 expression, female flies expressing RFP-  
610 tagged histones and GFP-tagged MCP (yw; His-RFP/Cyo; MCP-GFP/TM3.Sb) were crossed with  
611 males containing one of the MS2 reporter constructs.

### 612 613 **Sample preparation and image acquisition**

614 As in Garcia et al., live embryos were collected prior to nuclear cycle 14 (nc14), dechorionated,  
615 mounted with glue on a permeable membrane, immersed in Halocarbon 27 oil, and put under a  
616 glass coverslip (Garcia et al., 2013). Individual embryos were then imaged on a Nikon A1R point  
617 scanning confocal microscope using a 60X/1.4 N.A. oil immersion objective and laser settings of  
618 40uW for 488 nm and 35uW for 561 nm. To track transcription, 21 slice Z-stacks, at 0.5 um steps,  
619 were taken throughout nc14 at roughly 30s intervals. To identify the Z-stack's position in the  
620 embryo, the whole embryo was imaged at the end of nc14 at 20x using the same laser power  
621 settings. To quantify expression along the AP axis, each transcriptional spot's location was placed  
622 in 2.5% anterior-posterior (AP) bins across the length of the embryo, with the first bin at the  
623 anterior of the embryo. Embryos were imaged at ambient temperature, which was on average  
624 26.5°C.

### 625 626 **Burst calling and calculation of transcription parameters**

627 Tracking of nuclei and transcriptional puncta was done using a version of the image analysis  
628 MATLAB pipeline downloaded from the Garcia lab GitHub repository on January 8, 2020 and  
629 described in Garcia et al (Garcia et al., 2013). For every spot of transcription imaged, background  
630 fluorescence at each time point is estimated as the offset of fitting the 2D maximum projection of  
631 the Z-stack image centered around the transcriptional spot to a gaussian curve, using MATLAB  
632 *lsqnonlin*. This background estimate is subtracted from the raw spot fluorescence intensity. The  
633 resulting fluorescence traces across nc14 are then smoothed by the LOWESS method with a  
634 span of 10%. These smoothed traces are then used to quantify transcriptional properties and  
635 noise. Traces consisting of fewer than three timeframes are not included in the calculations.

636 To quantify the transcription properties of interest, we used the smoothed traces to  
637 determine at which time points the promoter was “on” or “off” (Waymack et al., 2020). A promoter  
638 was considered “on” if the slope of its trace, i.e. the change in fluorescence, between one point  
639 and the next was greater than or equal to the instantaneous fluorescence value calculated for one  
640 mRNA molecule ( $F_{RNAP}$ , described below). Once called “on”, the promoter is considered active  
641 until the slope of the fluorescence trace becomes less than or equal to the negative instantaneous

642 fluorescence value of one mRNA molecule, at which point it is considered inactive until the next  
643 time point it is called “on”. The instantaneous fluorescence of a single mRNA was chosen as the  
644 threshold because we reasoned that an increase in fluorescence greater than or equal to that of  
645 a single transcript is indicative of an actively producing promoter, just as a decrease in  
646 fluorescence greater than that associated with a single transcript indicates that transcripts are  
647 primarily dissociating from, not being newly initiated at, this locus. Visual inspection of  
648 fluorescence traces agreed well with the burst calling produced by this method (Figure S4)  
649 (Waymack et al., 2020).

650 Using these smoothed traces and “on” and “off” time points of promoters, we measured  
651 burst size, burst frequency, burst duration, polymerase initiation rate, and noise. Burst size is  
652 defined as the integrated area under the curve of each transcriptional burst, from one “on” frame  
653 to the next “on” frame, with the value of 0 set to the floor of the background-subtracted  
654 fluorescence trace (Figure S4C). Frequency is defined as the number of bursts in nc14 divided  
655 by time between the first time the promoter is called active and 50 min into nc14 or the movie  
656 ends, whichever is first (Figure S4E). The time of first activity was used for frequency calculations  
657 because the different enhancer constructs showed different characteristic times to first  
658 transcriptional burst during nc14. Duration is defined as the amount of time occurring between  
659 the frame a promoter is considered “on” and the frame it is next considered “off” (Figure S4F).  
660 Polymerase initiation rate is defined as the slope at the midpoint between the frame a promoter  
661 is considered “on” and the frame it is next considered “off” (Figure S4G). The temporal coefficient  
662 of variation of each transcriptional spot  $i$ , was calculated using the formula:  
663

$$664 CV(i) = \frac{\text{standard deviation } (m_i(t))}{\text{mean}_i(m(t))}$$

665  
666 where  $m_i(t)$  is the fluorescence of spot  $i$  at time  $t$ . For these, and all other measurements, we  
667 control for the embryo position of the fluorescence trace by first individually analyzing the trace  
668 and then using all the traces in each AP bin (anterior-posterior; the embryo is divided into 41 bins  
669 each containing 2.5% of the embryo’s length) to calculate summary statistics of the transcriptional  
670 dynamics and noise values at that AP position.

671 All original MATLAB code used for burst calling, noise measurements, and other image  
672 processing are available at the Wunderlich Lab GitHub (Waymack et al., 2020) with a copy  
673 archived at <https://github.com/elifeosciences-publications/KrShadowEnhancerCode>. Updates to  
674 include calculations of polymerase initiation rate are also available at the Wunderlich Lab GitHub  
675 (<https://github.com/WunderlichLab>).  
676

## 677 **Conversion of integrated fluorescence to mRNA molecules**

678 To convert arbitrary fluorescence units into physiologically relevant units, we calibrated our  
679 fluorescence measurements in terms of mRNA molecules. As in Lammers et al., for our  
680 microscope, we determined a calibration factor,  $\alpha$ , between our MS2 signal integrated over nc13,  
681  $F_{MS2}$ , and the number of mRNAs generated by a single allele from the same reporter construct in  
682 the same time interval,  $N_{FISH}$ , using the *hunchback* P2 enhancer reporter construct (Garcia et al.,  
683 2013; Lammers et al., 2020). Using this conversion factor, we calculated the integrated  
684 fluorescence of a single mRNA ( $F_1$ ) as well as the instantaneous fluorescence of an mRNA

685 molecule ( $F_{RNAP}$ ). For our microscope,  $F_{RNAP}$  is 379 AU/RNAP, and  $F_1$  is 1338 AU/RNAP·min. We  
686 can use these values to convert both integrated and instantaneous fluorescence into total mRNAs  
687 produced and number of nascent mRNAs present at a single time point, by dividing by  $F_1$  and  
688  $F_{RNAP}$ , respectively.

689

## 690 **Regression modeling and statistical analysis**

691 To quantify the effect of enhancer, promoter, and interaction terms on burst parameters, we  
692 considered models of the form

693

694 
$$g(Y) = \text{enhancer} + \text{promoter} + (\text{enhancer} \times \text{promoter})$$

695

696 where  $Y$  is the burst property of interest and  $g$  is the link function (Figure 4A). Model selection  
697 involved considering (1) the type of model, (2) the distribution that best fit the burst property data  
698 and (3) the appropriate predictors to include. We approached model selection with no specific  
699 expectations, opting to use generalized linear models (GLMs) because they were not much  
700 improved upon by adding random effects (GLMMs) and because they fit the data better than linear  
701 models (LMs).

702 Similarly, the appropriate distribution for each burst property was determined by fitting  
703 various distributions to the data and comparing their goodness-of-fit. As expected, total RNA  
704 produced and burst size (in transcripts per burst) were best described by a negative binomial  
705 distribution, as has been commonly used to describe count data. For the other burst properties,  
706 for which the appropriate distribution was less clear, we found that burst frequency was best fit  
707 by the Weibull distribution and burst duration and initiation rate were best fit by the gamma  
708 distribution. These choices were supported by the lower AIC values produced when comparing  
709 them to models using alternative distributions. They also seem reasonable given examples of  
710 other applications of these distributions. To keep the interpretation consistent across models, we  
711 chose to use an identity link function for all models (Figure 4B); using the canonical link functions  
712 associated with each of these distributions produced the same trends (Figure S5).

713 The predictors we included were the enhancer and promoter and any interaction terms  
714 between the enhancer and promoter. In each case, dropping the interaction terms produced  
715 higher AIC values, suggesting that the interaction terms are important and should not be dropped  
716 by the model.

717 To determine any significant differences in mean expression levels, we performed Welch's  
718 *t*-tests, and to determine if any predictors led to significant differences in burst duration, we  
719 performed a multivariate ANOVA. To quantify the variability explained by different predictors, we  
720 calculated the Cragg and Uhler pseudo R-squared measures of the model including only the  
721 predictor in question and divided by that of the full model described above.

722

## 723 **Data Availability Statement**

724 Transgenic fly strains and plasmids are available upon request. Supplementary File S1 contains  
725 the gene names, the dm6 release coordinates, and the FlyBase numbers (FBgn) that matched  
726 to the gene names and coordinates (Corrales et al., 2017). File S2 contains DNA sequences of  
727 the enhancers and promoters used in the computational analysis presented in Figure S2. Files

728 S3-18 contain GenBank files describing the plasmids used to make all the transgenic fly strains  
729 produced for this work.

730

## 731 References

732 Batut, P., Dobin, A., Plessy, C., Carninci, P., & Gingeras, T. R. (2013). High-fidelity promoter  
733 profiling reveals widespread alternative promoter usage and transposon-driven  
734 developmental gene expression. *Genome Research*, 23(1), 169–180.  
735 <https://doi.org/10.1101/gr.139618.112>

736 Batut, P. J., & Gingeras, T. R. (2017). Conserved noncoding transcription and core promoter  
737 regulatory code in early *Drosophila* development. *eLife*, 6, 156596.  
738 <https://doi.org/10.7554/eLife.29005>

739 Bonn, S., Zinzen, R. P., Girardot, C., Gustafson, E. H., Perez-Gonzalez, A., Delhomme, N., ...  
740 Furlong, E. E. M. (2012). Tissue-specific analysis of chromatin state identifies temporal  
741 signatures of enhancer activity during embryonic development. *Nature Genetics*, 44(2),  
742 148–156. <https://doi.org/10.1038/ng.1064>

743 Bothma, J. P., Garcia, H. G., Ng, S., Perry, M. W., Gregor, T., & Levine, M. (2015). Enhancer  
744 additivity and non-additivity are determined by enhancer strength in the *Drosophila* embryo.  
745 *eLife*, 4(AUGUST2015). <https://doi.org/10.7554/eLife.07956>

746 Brown, J. B., Boley, N., Eisman, R., May, G. E., Stoiber, M. H., Duff, M. O., ... Celniker, S. E.  
747 (2014). Diversity and dynamics of the *Drosophila* transcriptome. *Nature*, 512(7515), 393–  
748 399. <https://doi.org/10.1038/nature12962>

749 Burke, T. W., & Kadonaga, J. T. (1996). *Drosophila* TFIID binds to a conserved downstream  
750 basal promoter element that is present in many TATA-box-deficient promoters. *Genes and  
751 Development*, 10(6), 711–724. <https://doi.org/10.1101/gad.10.6.711>

752 Chalkley, G. E., & Verrijzer, C. P. (1999). DNA binding site selection by RNA polymerase II  
753 TAFs: A TAF(II)250-TAF(II)150 complex recognizes the initiator. *EMBO Journal*, 18(17),  
754 4835–4845. <https://doi.org/10.1093/emboj/18.17.4835>

755 Corrales, M., Rosado, A., Cortini, R., van Arensbergen, J., van Steensel, B., & Filion, G. J.  
756 (2017). Clustering of *Drosophila* housekeeping promoters facilitates their expression.  
757 *Genome Research*, 27(7), 1153–1161. <https://doi.org/10.1101/gr.211433.116>

758 Dar, R. D., Razooky, B. S., Singh, A., Trimeloni, T. V., McCollum, J. M., Cox, C. D., ...  
759 Weinberger, L. S. (2012). Transcriptional burst frequency and burst size are equally  
760 modulated across the human genome. *Proceedings of the National Academy of Sciences  
761 of the United States of America*, 109(43), 17454–17459.  
762 <https://doi.org/10.1073/pnas.1213530109>

763 Dreos, R., Ambrosini, G., Cavin Périer, R., & Bucher, P. (2013). EPD and EPDnew, high-quality  
764 promoter resources in the next-generation sequencing era. *Nucleic Acids Research*,  
765 41(Database issue), D157-64. <https://doi.org/10.1093/nar/gks1233>

766 Dreos, R., Ambrosini, G., Groux, R., Cavin Périer, R., & Bucher, P. (2016). The eukaryotic  
767 promoter database in its 30th year: focus on non-vertebrate organisms. *Nucleic Acids  
768 Research*, 45(November 2016), gkw1069. <https://doi.org/10.1093/NAR/GKW1069>

769 El-Sherif, E., & Levine, M. (2016). Shadow Enhancers Mediate Dynamic Shifts of Gap Gene  
770 Expression in the *Drosophila* Embryo. *Current Biology : CB*, 26(9), 1164–1169.  
771 <https://doi.org/10.1016/j.cub.2016.02.054>

772 Emami, K. H., Jain, A., & Smale, S. T. (1997). Mechanism of synergy between TATA and  
773 initiator: Synergistic binding of TFIID following a putative TFIIA-induced isomerization.  
774 *Genes and Development*, 11(22), 3007–3019. <https://doi.org/10.1101/gad.11.22.3007>

775 Falo-Sanjuan, J., Lammers, N. C., Garcia, H. G., & Bray, S. J. (2019). Enhancer Priming  
776 Enables Fast and Sustained Transcriptional Responses to Notch Signaling. *Developmental*

777 *Cell*, 50(4), 411–425.e8. <https://doi.org/10.1016/j.devcel.2019.07.002>

778 Fukaya, T., Lim, B., & Levine, M. (2016). Enhancer Control of Transcriptional Bursting. *Cell*,  
779 166(2), 358–368. <https://doi.org/10.1016/j.cell.2016.05.025>

780 Garcia, H. G., Tikhonov, M., Lin, A., & Gregor, T. (2013, November 4). Quantitative Imaging of  
781 Transcription in Living Drosophila Embryos Links Polymerase Activity to Patterning.  
782 *Current Biology*, pp. 2140–2145. <https://doi.org/10.1016/j.cub.2013.08.054>

783 Gehrig, J., Reischl, M., Kalmár, E., Ferg, M., Hadzhiev, Y., Zaucker, A., ... Müller, F. (2009).  
784 Automated high-throughput mapping of promoter-enhancer interactions in zebrafish  
785 embryos. *Nature Methods*, 6(12), 911–916. <https://doi.org/10.1038/nmeth.1396>

786 Ghavi-Helm, Y., Klein, F. A., Pakozdi, T., Ciglar, L., Noordermeer, D., Huber, W., & Furlong, E.  
787 E. M. (2014). Enhancer loops appear stable during development and are associated with  
788 paused polymerase. *Nature*, 512(7512), 96–100. <https://doi.org/10.1038/nature13417>

789 Halfon, M. S., Gallo, S. M., & Bergman, C. M. (2008). REDfly 2.0: an integrated database of cis-  
790 regulatory modules and transcription factor binding sites in Drosophila. *Nucleic Acids  
791 Research*, 36(Database issue), D594–D598. <https://doi.org/10.1093/nar/gkm876>

792 Hansen, S. K., Takada, S., Jacobson, R. H., Lis, J. T., & Tjian, R. (1997). Transcription  
793 properties of a cell type-specific TATA-binding protein, TRF. *Cell*, 91(1), 71–83.  
794 [https://doi.org/10.1016/S0092-8674\(01\)80010-6](https://doi.org/10.1016/S0092-8674(01)80010-6)

795 Hendy, O., Campbell, J., Weissman, J. D., Larson, D. R., & Singer, D. S. (2017). Differential  
796 context-specific impact of individual core promoter elements on transcriptional dynamics.  
797 *Molecular Biology of the Cell*, 28(23), 3360–3370. <https://doi.org/10.1091/mbc.E17-06-0408>

798 Hertz, G. Z., & Stormo, G. D. (1999). Identifying DNA and protein patterns with statistically  
799 significant alignments of multiple sequences. *Bioinformatics (Oxford, England)*, 15(7–8),  
800 563–577. <https://doi.org/10.1093/bioinformatics/15.7.563>

801 Holmes, M. C., & Tjian, R. (2000). Promoter-selective properties of the TBP-related factor  
802 TRF1. *Science*, 288(5467), 867–870. <https://doi.org/10.1126/science.288.5467.867>

803 Hoppe, C., Bowles, J. R., Minchington, T. G., Sutcliffe, C., Upadhyai, P., Rattray, M., & Ashe, H.  
804 L. (2020). Modulation of the Promoter Activation Rate Dictates the Transcriptional  
805 Response to Graded BMP Signaling Levels in the Drosophila Embryo. *Developmental Cell*,  
806 54(6), 727–741.e7. <https://doi.org/10.1016/j.devcel.2020.07.007>

807 Hsu, J. Y., Juven-Gershon, T., Marr, M. T., Wright, K. J., Tjian, R., & Kadonaga, J. T. (2008).  
808 TBP, Mot1, and NC2 establish a regulatory circuit that controls DPE-dependent versus  
809 TATA-dependent transcription. *Genes and Development*, 22(17), 2353–2358.  
810 <https://doi.org/10.1101/gad.1681808>

811 Juven-Gershon, T., Hsu, J. Y., & Kadonaga, J. T. (2008). Caudal, a key developmental  
812 regulator, is a DPE-specific transcriptional factor. *Genes and Development*, 22(20), 2823–  
813 2830. <https://doi.org/10.1101/gad.1698108>

814 Juven-Gershon, T., Hsu, J. Y., Theisen, J. W., & Kadonaga, J. T. (2008). The RNA polymerase  
815 II core promoter - the gateway to transcription. *Current Opinion in Cell Biology*, 20(3), 253–  
816 259. <https://doi.org/10.1016/j.ceb.2008.03.003>

817 Kim, J. L., Nikolov, D. B., & Burley, S. K. (1993). Co-crystal structure of TBP recognizing the  
818 minor groove of a TATA element. *Nature*, 365(6446), 520–527.  
819 <https://doi.org/10.1038/365520a0>

820 Kvon, E. Z., Kazmar, T., Stampfel, G., Yáñez-Cuna, J. O., Pagani, M., Schernhuber, K., ...  
821 Stark, A. (2014). Genome-scale functional characterization of Drosophila developmental  
822 enhancers in vivo. *Nature*, 512(7512), 91–95. <https://doi.org/10.1038/nature13395>

823 Kvon, E. Z., Waymack, R., Elabd, M. G., & Wunderlich, Z. (2021). Enhancer redundancy in  
824 development and disease. *Nature Reviews Genetics*. <https://doi.org/10.1038/s41576-020-00311-x>

825 Lammers, N. C., Galstyan, V., Reimer, A., Medin, S. A., Wiggins, C. H., & Garcia, H. G. (2020).  
826

827

828 Multimodal transcriptional control of pattern formation in embryonic development.  
829 *Proceedings of the National Academy of Sciences of the United States of America*, 117(2),  
830 836–847. <https://doi.org/10.1073/pnas.1912500117>

831 Landry, J. R., Mager, D. L., & Wilhelm, B. T. (2003). Complex controls: The role of alternative  
832 promoters in mammalian genomes. *Trends in Genetics*, 19(11), 640–648.  
833 <https://doi.org/10.1016/j.tig.2003.09.014>

834 Larsson, A. J. M., Johnsson, P., Hagemann-Jensen, M., Hartmanis, L., Faridani, O. R., Reinius,  
835 B., ... Sandberg, R. (2019). Genomic encoding of transcriptional burst kinetics. *Nature*,  
836 565(7738), 251–254. <https://doi.org/10.1038/s41586-018-0836-1>

837 Lee, C. H., Shin, H., & Kimble, J. (2019). Dynamics of Notch-Dependent Transcriptional  
838 Bursting in Its Native Context. *Developmental Cell*, 50(4), 426–435.e4.  
839 <https://doi.org/10.1016/j.devcel.2019.07.001>

840 Lewis, B. A., Sims, R. J., Lane, W. S., & Reinberg, D. (2005). Functional characterization of  
841 core promoter elements: DPE-specific transcription requires the protein kinase CK2 and  
842 the PC4 coactivator. *Molecular Cell*, 18(4), 471–481.  
843 <https://doi.org/10.1016/j.molcel.2005.04.005>

844 Lim, B., & Levine, M. S. (2021). Enhancer-promoter communication: hubs or loops? *Current  
845 Opinion in Genetics and Development*, 67, 5–9. <https://doi.org/10.1016/j.gde.2020.10.001>

846 Ling, J., Umezawa, K. Y., Scott, T., & Small, S. (2019). Bicoid-Dependent Activation of the  
847 Target Gene hunchback Requires a Two-Motif Sequence Code in a Specific Basal  
848 Promoter. *Molecular Cell*, 1–10. <https://doi.org/10.1016/j.molcel.2019.06.038>

849 Lott, S. E., Villalta, J. E., Schroth, G. P., Luo, S., Tonkin, L. A., & Eisen, M. B. (2011).  
850 Noncanonical compensation of zygotic X transcription in early *Drosophila melanogaster*  
851 development revealed through single-embryo RNA-Seq. *PLoS Biology*, 9(2).  
852 <https://doi.org/10.1371/journal.pbio.1000590>

853 Pankratz, M. J., Busch, M., Hoch, M., Seifert, E., Pankratz, M. J., Busch, M., ... Jackle, H.  
854 (1992). Spatial Control of the Gap Gene knirps in the *Drosophila* Embryo by Posterior  
855 Morphogen System Herbert Jäckle Published by : American Association for the  
856 Advancement of Science Stable URL : <http://www.jstor.org/stable/2876592> digitize ,  
857 preserve and extend. *Science*, 255(5047), 986–989.  
858 <https://doi.org/10.1126/science.1546296>

859 Patro, R., Duggal, G., Love, M. I., Irizarry, R. A., & Kingsford, C. (2017). Salmon provides fast  
860 and bias-aware quantification of transcript expression. *Nature Methods*, 14(4), 417–419.  
861 <https://doi.org/10.1038/nmeth.4197>

862 Peccoud, J., & Ycart, B. (1995). Markovian modeling of gene-product synthesis. *Theoretical  
863 Population Biology*. <https://doi.org/10.1006/tpbi.1995.1027>

864 Pelegri, F., & Lehmann, R. (1994). A role of polycomb group genes in the regulation of gap  
865 gene expression in *Drosophila*. *Genetics*, 136(4), 1341–1353.  
866 <https://doi.org/10.1093/genetics/136.4.1341>

867 Perry, M. W., Boettiger, A. N., & Levine, M. (2011). Multiple enhancers ensure precision of gap  
868 gene-expression patterns in the *Drosophila* embryo. *Proceedings of the National Academy  
869 of Sciences of the United States of America*, 108(33), 13570–13575.  
870 <https://doi.org/10.1073/pnas.1109873108>

871 Pimmett, V., Dejean, M., Fernandez, C., Trullo, A., Betrand, E., Radulescu, O., & Lagha, M.  
872 (2021). Quantitative imaging of transcription in living *Drosophila* embryos reveals the  
873 impact of core promoter motifs on promoter state dynamics. *BioRxiv*.  
874 <https://doi.org/https://doi.org/10.1101/2021.01.22.427786>

875 Qin, J. Y., Zhang, L., Clift, K. L., Hulur, I., Xiang, A. P., Ren, B. Z., & Lahn, B. T. (2010).  
876 Systematic comparison of constitutive promoters and the doxycycline-inducible promoter.  
877 *PLoS ONE*, 5(5), 3–6. <https://doi.org/10.1371/journal.pone.0010611>

878 Ramalingam, V., Natarajan, M., Johnston, J., & Zeitlinger, J. (2021). TATA and paused

879 promoters active in differentiated tissues have distinct expression characteristics.  
880 *Molecular Systems Biology*, 17(2), 1–12. <https://doi.org/10.1525/msb.20209866>

881 Ravarani, C. N. J., Chalancon, G., Breker, M., de Groot, N. S., & Babu, M. M. (2016). Affinity  
882 and competition for TBP are molecular determinants of gene expression noise. *Nature  
883 Communications*, 7, 10417. <https://doi.org/10.1038/ncomms10417>

884 Schibler, U., & Sierra, F. (1987). Alternative Promoters in Developmental Gene Expression.  
885 *Annual Review of Genetics*, 21(1), 237–257.  
886 <https://doi.org/10.1146/annurev.ge.21.120187.001321>

887 Schröder, C., Tautz, D., Seifert, E., & Jäckle, H. (1988). Differential regulation of the two  
888 transcripts from the *Drosophila* gap segmentation gene *hunchback*. *The EMBO Journal*,  
889 7(9), 2881–2887. Retrieved from  
890 <http://www.pubmedcentral.nih.gov/articlerender.fcgi?artid=457082&tool=pmcentrez&render=abstract>

891 Schroeder, M. D., Pearce, M., Fak, J., Fan, H. Q., Unnerstall, U., Emberly, E., ... Gaul, U.  
892 (2004). Transcriptional control in the segmentation gene network of *Drosophila*. *PLoS  
893 Biology*, 2(9), E271. <https://doi.org/10.1371/journal.pbio.0020271>

894 Senecal, A., Munsky, B., Proux, F., Ly, N., Braye, F. E., Zimmer, C., ... Darzacq, X. (2014).  
895 Transcription factors modulate c-Fos transcriptional bursts. *Cell Reports*, 8(1), 75–83.  
896 <https://doi.org/10.1016/j.celrep.2014.05.053>

897 Shao, H., Revach, M., Moshonov, S., Tzuman, Y., Gazit, K., Albeck, S., ... Dikstein, R. (2005).  
898 Core Promoter Binding by Histone-Like TAF Complexes. *Molecular and Cellular Biology*,  
899 25(1), 206–219. <https://doi.org/10.1128/mcb.25.1.206-219.2005>

900 Sloutskin, A., Danino, Y. M., Orenstein, Y., Zehavi, Y., Doniger, T., Shamir, R., & Juven-  
901 Gershon, T. (2015). ElemeNT: a computational tool for detecting core promoter elements.  
902 *Transcription*, 6(3), 41–50. <https://doi.org/10.1080/21541264.2015.1067286>

903 Tunnacliffe, E., & Chubb, J. R. (2020). What Is a Transcriptional Burst? *Trends in Genetics*,  
904 36(4), 288–297. <https://doi.org/10.1016/j.tig.2020.01.003>

905 van Arensbergen, J., van Steensel, B., & Bussemaker, H. J. (2014). In search of the  
906 determinants of enhancer-promoter interaction specificity. *Trends in Cell Biology*, 24(11),  
907 695–702. <https://doi.org/10.1016/j.tcb.2014.07.004>

908 Vo Ngoc, L., Wang, Y.-L., Kassavetis, G. A., & Kadonaga, J. T. (2017). The punctilious RNA  
909 polymerase II core promoter. *Genes & Development*, 31(13), 1289–1301.  
910 <https://doi.org/10.1101/gad.303149.117>

911 Wang, X., Hou, J., Quedenau, C., & Chen, W. (2016). Pervasive isoform-specific translational  
912 regulation via alternative transcription start sites in mammals. *Molecular Systems Biology*,  
913 12(7), 875. <https://doi.org/10.1525/msb.20166941>

914 Waymack, R., Fletcher, A., Enciso, G., & Wunderlich, Z. (2020). Shadow enhancers can  
915 suppress input transcription factor noise through distinct regulatory logic. *ELife*, 9, 1–57.  
916 <https://doi.org/10.7554/ELIFE.59351>

917 Wu, C.-H. H., Madabusi, L., Nishioka, H., Emanuel, P., Sypes, M., Arkhipova, I., & Gilmour, D.  
918 S. (2001). Analysis of Core Promoter Sequences Located Downstream from the TATA  
919 Element in the. *Society*, 21(5), 1593–1602. <https://doi.org/10.1128/MCB.21.5.1593>

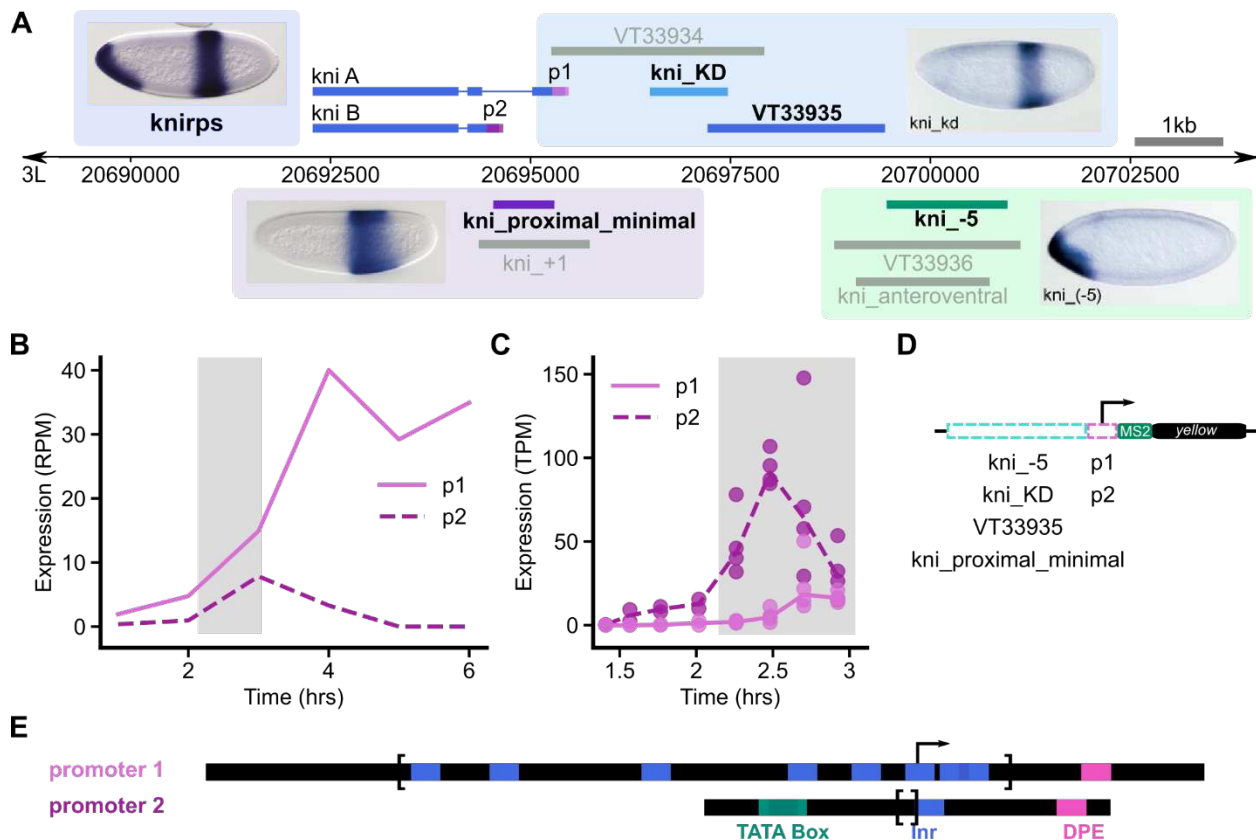
920 Wunderlich, Z., Bragdon, M. D., Eckenrode, K. B., Lydiard-Martin, T., Pearl-Waserman, S., &  
921 Depace, A. H. (2012). Dissecting sources of quantitative gene expression pattern  
922 divergence between *Drosophila* species. *Molecular Systems Biology*, 8(604), 604.  
923 <https://doi.org/10.1038/msb.2012.35>

924 Yokoshi, M., Cambón, M., & Fukaya, T. (2021). Regulation of transcriptional bursting by core  
925 promoter elements in the *Drosophila* embryo. *BioRxiv*.  
926 <https://doi.org/https://doi.org/10.1101/2021.03.18.435761>

927 Zehavi, Y., Kuznetsov, O., Ovadia-Shochat, A., & Juven-Gershon, T. (2014). Core Promoter  
928 Functions in the Regulation of Gene Expression of *Drosophila* Dorsal Target Genes.  
929

930        *Journal of Biological Chemistry*, 289(17), 11993–12004.  
931        <https://doi.org/10.1074/jbc.M114.550251>  
932        Zhu, L. J., Christensen, R. G., Kazemian, M., Hull, C. J., Enuameh, M. S., Basciotta, M. D., ...  
933        Brodsky, M. H. (2011). FlyFactorSurvey: A database of *Drosophila* transcription factor  
934        binding specificities determined using the bacterial one-hybrid system. *Nucleic Acids*  
935        *Research*, 39(SUPPL. 1), 111–117. <https://doi.org/10.1093/nar/gkq858>  
936        Zoller, B., Little, S. C., & Gregor, T. (2018). Diverse Spatial Expression Patterns Emerge from  
937        Unified Kinetics of Transcriptional Bursting. *Cell*, 175(3), 835-847.e25.  
938        <https://doi.org/10.1016/j.cell.2018.09.056>  
939  
940

941 **Figures**



942  
943 **Figure 1. knirps as a case study.** The *knirps* (*kni*) locus was chosen to study how the motif  
944 content of endogenous enhancers and promoters affects transcription dynamics. This locus was  
945 selected because it comprises multiple enhancers that bind different TFs and multiple core  
946 promoters that contain different promoter motifs. These enhancers and promoters are all active  
947 during the blastoderm stage.

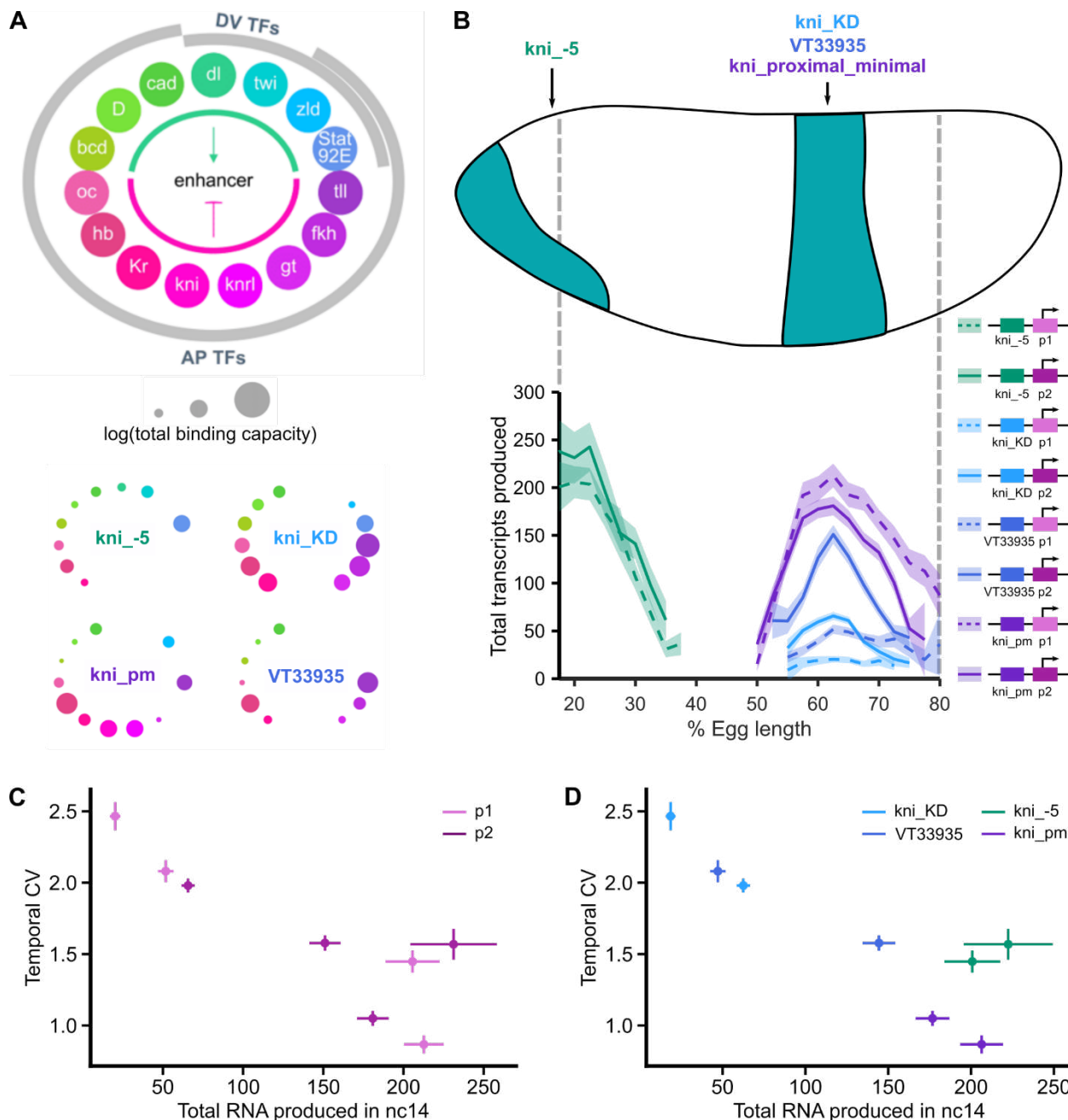
948 **(A)** The *kni* locus comprises multiple enhancers that together drive expression of a ventral,  
949 anterior band and a posterior stripe, as shown in the *in situ* at the top left. Enhancers that drive  
950 similar expression patterns have been displayed together in boxes with a representative *in situ*  
951 hybridization (Perry et al., 2011; Schroeder et al., 2004). The four enhancers selected for study  
952 are in color and labeled in bold text; the others are in gray. *kni* also has two promoters represented  
953 in two shades of purple, which drive slightly different transcripts (differing by only five amino  
954 acids). Expression data for the two *kni* promoters is shown, with RAMPAGE data (P. J. Batut &  
955 Gingeras, 2017) in **(B)** and RNA-seq data (Lott et al., 2011) in **(C)**; the time period corresponding  
956 to the blastoderm stage is highlighted in gray. Based on these two sets of data, the two *kni*  
957 promoters are both used during nuclear cycle 14 though which one is more active is less clear.  
958 Note that for the rest of development, promoter 1 is the more active one. **(D)** A total of eight MS2  
959 reporter constructs containing pairs of each of the four enhancers matched with each of the two  
960 *kni* promoters were made. **(E)** The two *kni* promoters are shown here in black, consisting of the  
961 RAMPAGE-defined transcription start clusters (TSCs) between the brackets and an additional  $\pm$   
962 40bp from the TSCs. The two *kni* promoters can be distinguished by their motif content (with  
963 promoter 1 consisting of a series of Inr motifs and a DPE motif and promoter 2 consisting of an

964 Inr, two overlapping TATA Boxes and a DPE motif). They also differ in the “sharpness” of their  
965 region of transcription initiation (shown between the brackets), with promoter 1 (124bp) being  
966 significantly broader than promoter 2 (3bp) based on RAMPAGE tag data (P. J. Batut & Gingeras,  
967 2017).

968

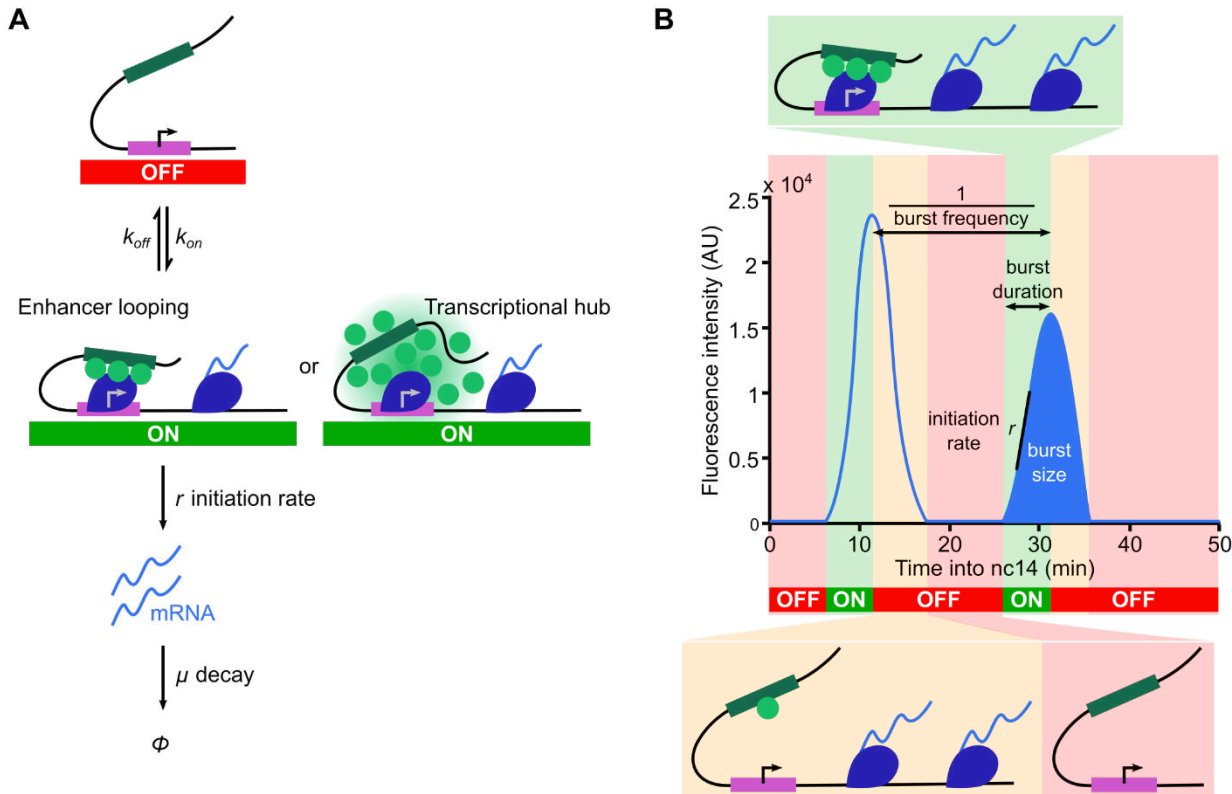
969

970



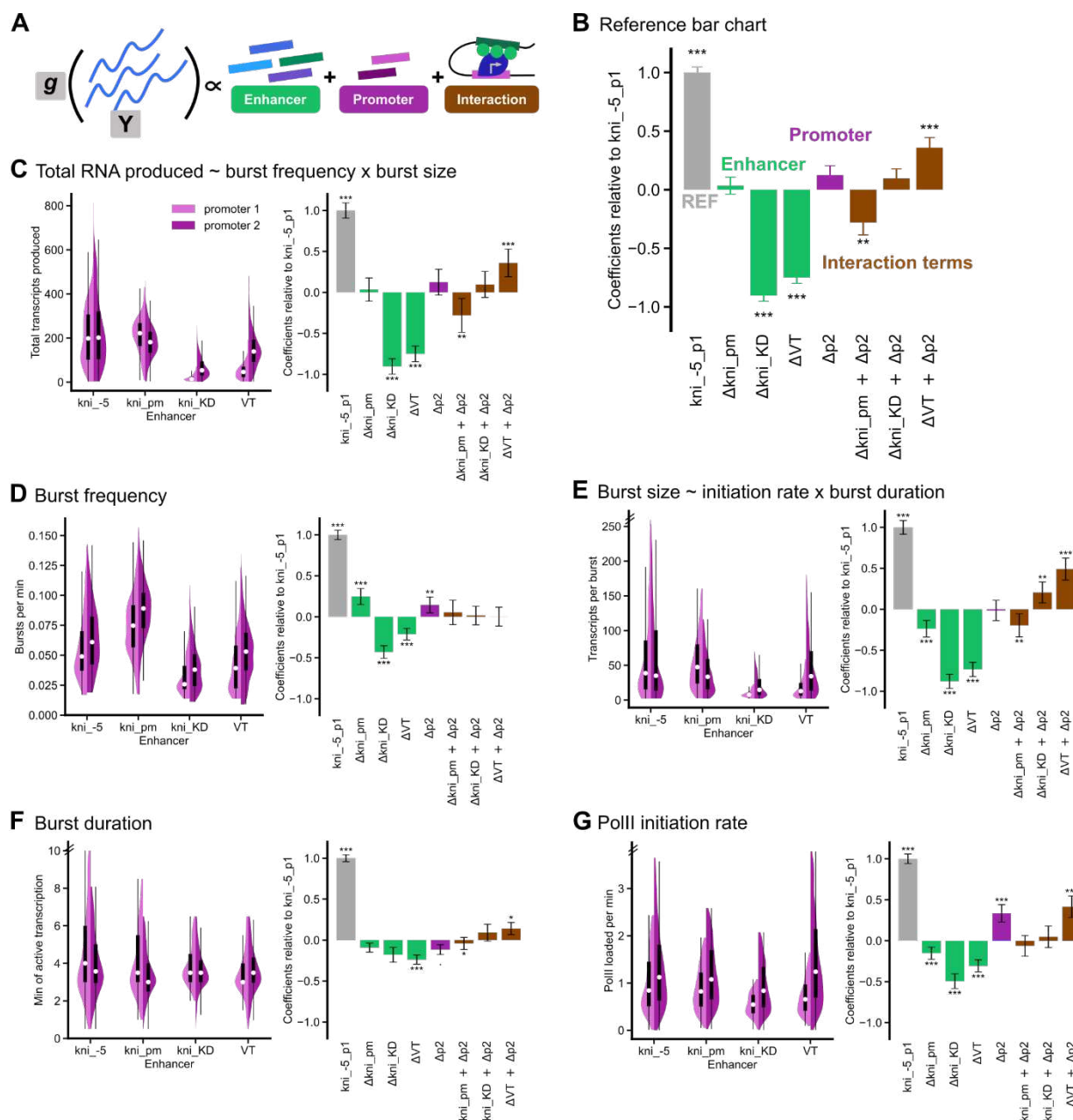
971 **Figure 2. The *kni* enhancers differ in their capacity to bind different transcription factors**  
972 **and drive transcription with different promoters.** The enhancers can be separated into two  
973 classes—those that produce high expression with either promoter (kni-5 and  
974 kni\_pm) and those that produce much higher expression with promoter 2 (kni\_KD  
975 and VT33935). Note that for simplicity, kni\_pm has been shortened to kni\_pm in  
976 the figures.  
977 **(A)** Here ability of the *kni* enhancers to bind early axis-patterning TFs is quantified and  
978 represented visually. The logarithm of the predicted TF binding capacity of each of the *kni*  
979 enhancers is plotted as circles around the enhancer, with the color indicating the TF and the circle  
980 size increasing with higher binding capacity. The TFs are categorized by their role in regulating  
981

982 anterior-posterior (AP) or dorsal-ventral (DV) patterning and broadly by their roles as activators  
983 (indicated by the green arc) and repressors (indicated by the pink arc). Note that kni\_KD and  
984 VT33935, which drive the same posterior stripe of expression, share very similar TFs and that  
985 kni\_-5, the only enhancer with a DV component, is the only one bound by DV TFs.  
986 Kni\_proximal\_minimal drives a similar expression pattern to kni\_KD and VT33935, but notably  
987 has different predicted TF binding capacities. **(B)** The *Drosophila* embryo with the *kni* expression  
988 pattern at nuclear cycle 14 is shown; kni\_-5 drives the expression of the anterior, ventral band,  
989 while the other three enhancers drive the expression of the posterior stripe. We made enhancer-  
990 promoter reporters containing each of the four enhancers matched with either promoter 1 or 2.  
991 Using measurements from these enhancer-promoter reporters (shown at the right), the total RNA  
992 produced by each construct during nuclear cycle 14 is plotted against position along the embryo  
993 length (AP axis). The error bands around the lines are 95% confidence intervals. The constructs  
994 containing promoter 1 are denoted with a dashed line and those containing promoter 2 with a  
995 solid line. Some, but not all, enhancers show a strong promoter preference. kni\_KD and VT33935,  
996 which are bound by similar TFs, drive 2.9-fold and 3.4-fold higher expression with promoter 2 at  
997 62.5% embryo length, respectively (one-sided *t*-test  $p < 2.2 \times 10^{-16}$  for both), whereas, kni\_-5 and  
998 kni\_proximal\_minimal show similar expression regardless of promoter with the largest difference  
999 only 1.2-fold at the anterior-posterior bin of maximum expression (22% and 63%, respectively)  
1000 (two-sided *t*-test comparing kni\_-5-promoter1 vs. kni\_-5-promoter2,  $p = 0.12$  and  
1001 kni\_proximal\_minimal-promoter1 vs. kni\_proximal\_minimal-promoter2  $p = 9.8 \times 10^{-5}$ ). In panels  
1002 **(C – D)**, the temporal coefficient of variation (CV) is plotted against the total RNA produced in  
1003 nc14 at the anterior-posterior bin of maximum expression (22% and 63%) for the anterior band  
1004 and the posterior stripe, respectively, with the error bars representing 95% confidence intervals.  
1005 There is a general trend of mean expression levels being anti-correlated with CV, or noise. **(C)**  
1006 Here, the data points are colored by the construct's promoter, with promoter 1 in light purple and  
1007 promoter 2 in purple. Despite the general trend, there are cases when the same promoter  
1008 (promoter 2) shows higher CV and total expression when paired with different enhancers  
1009 (kni\_proximal\_minimal vs kni\_-5). **(D)** Here, the data points are colored by the construct's  
1010 enhancer. Again, despite the general trend, there are cases when the same enhancer (kni\_-5)  
1011 shows higher CV and total expression when paired with different promoters (promoter 1 vs 2).  
1012  
1013  
1014



1015  
1016 **Figure 3. Two-state model of transcription in the context of tracking transcription**  
1017 **dynamics.**  
1018  
1019  
1020  
1021  
1022  
1023  
1024  
1025  
1026  
1027  
1028  
1029  
1030  
1031  
1032  
1033  
1034  
1035

(A) Here, we represent the two-state model of transcription, in which the promoter is either (1) in the inactive state (OFF), in which RNA polymerase cannot bind and initiate transcription or (2) in the active state (ON), during which it can. The promoter transitions between these two states with rates  $k_{on}$  and  $k_{off}$ , with promoter activation involving both the interaction of the enhancer and promoter and the assembly of all the necessary transcription machinery for transcription initiation to occur. This may occur through enhancer looping or through the formation of a transcriptional hub. In its active state, the promoter produces mRNA at rate  $r$ , and the mRNA decays by diffusing away from the gene locus at rate  $\mu$ . (B) MS2-tagging RNA allows us to track nascent transcription, and the resulting fluorescence trace (in light blue) is proportional to the number of nascent RNA produced over time. The graph is split into sections, representing different molecular states and how they correspond to fluctuating transcription over time. These states are represented by different colors—red when the promoter is OFF, green when it is ON, and yellow when transcription continues but the promoter is no longer ON, as no new polymerases are being loaded. The dynamics of these fluctuations or bursts can be characterized by quantifying various properties, including burst frequency (how often a burst occurs), burst size (number of RNA produced per burst), and burst duration (the period of active transcription during which mRNA is produced at rate  $r$ ).



1036

1037

#### Figure 4. Expression levels are mainly determined by burst frequency and initiation rate

1038

1039

1040

1041

1042

1043

1044

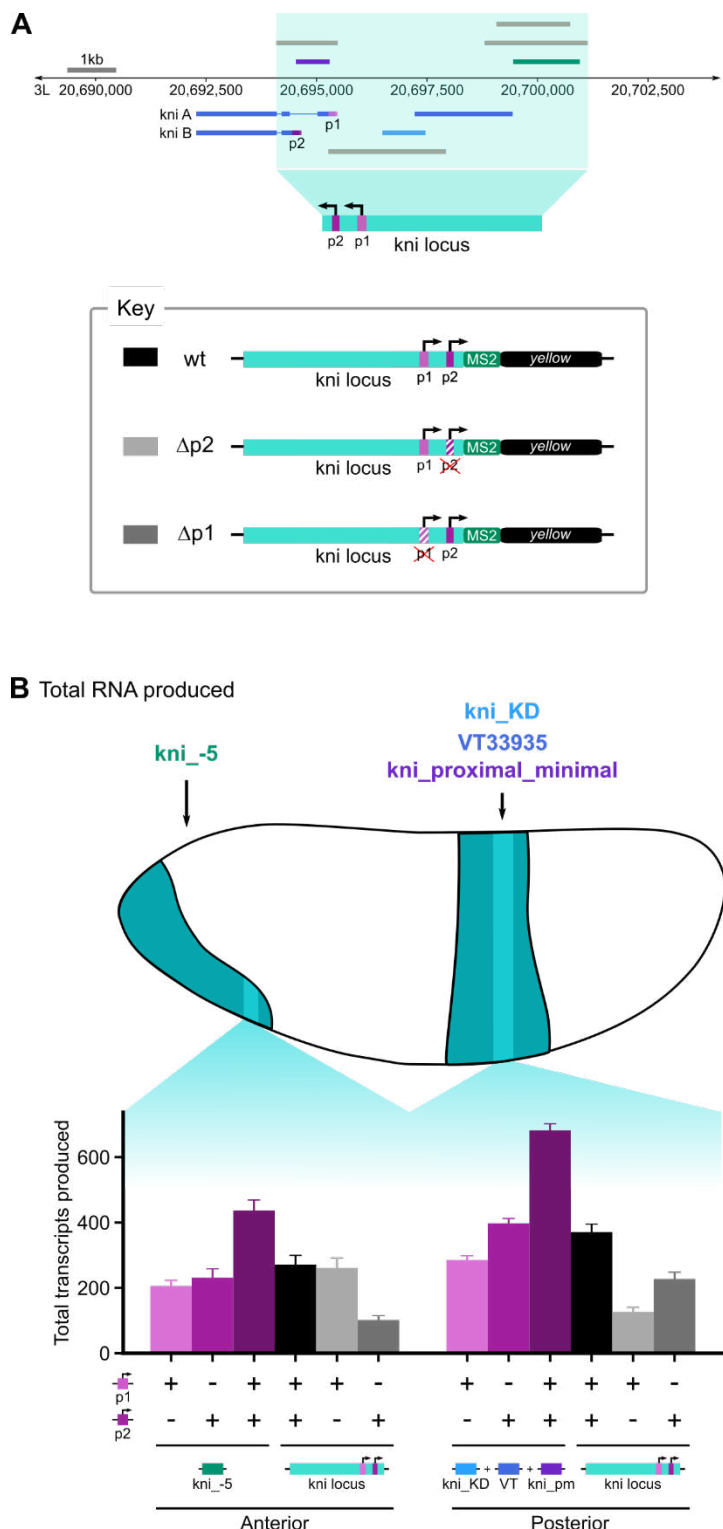
1045

1046

1047

(A) To parse the effects of the enhancer, the promoter, and their interactions on all burst properties, we built generalized linear models (GLMs). Y represents the burst property under study, g is the identity link function, and the enhancers, promoters, and their interaction terms are the explanatory variables. The coefficients of each of these explanatory variables is representative of that variable's contribution to the total value of the burst property. (B) All burst property data was taken from the anterior-posterior bin of maximum expression (22% and 63%) for the anterior band and the posterior stripe, respectively. The coefficients and the 95% confidence intervals for each independent variable relative to that of a reference construct (kni\_-5\_p1) are plotted as a bar graph; \*  $p < 0.05$ , \*\*  $p < 0.01$ , \*\*\*  $p < 0.001$ . The reference construct is represented in gray, and the effects of enhancer, promoter, and their interactions are represented

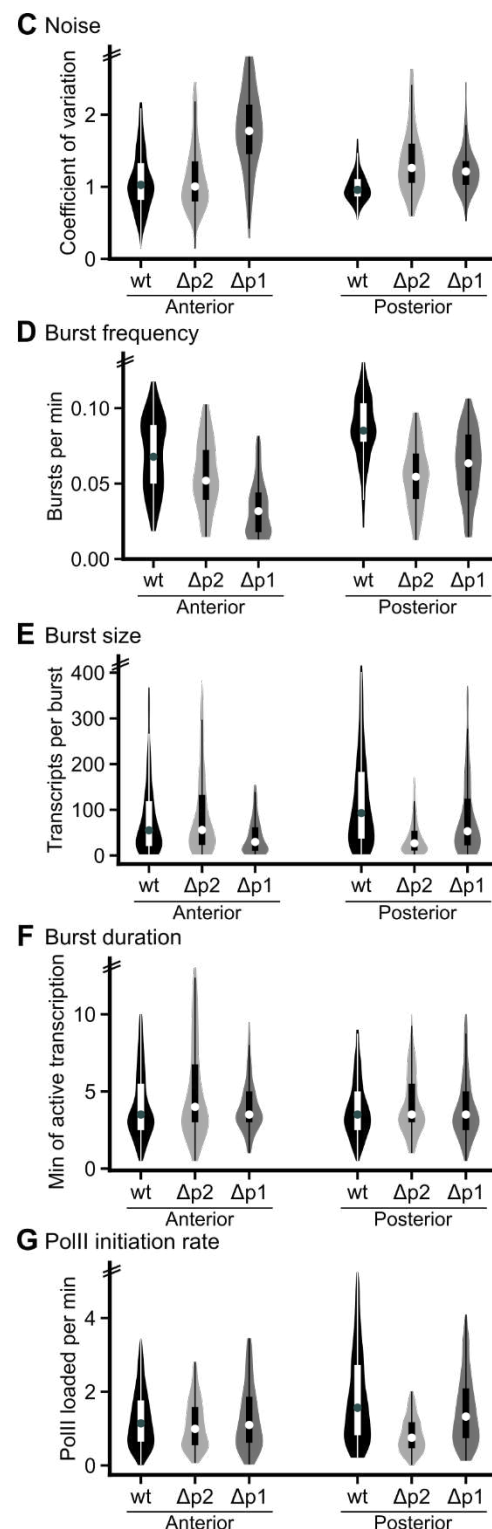
1048 in green, purple, and brown, respectively. Summing the relevant coefficients gives you the  
1049 average value of the burst property for a particular construct relative to the reference construct.  
1050 Thus, as the reference construct, kni\_-5-p1 coefficient will always be 1. The average value of the  
1051 burst property for a particular construct, e.g. VT-p2, relative to the reference construct, would be  
1052 0.75, which is the sum of the reference bar = 1,  $\Delta VT = -0.78$ ,  $\Delta p2 = 0.17$ , and  $\Delta VT + \Delta p2 = 0.36$ .  
1053 Note that for simplicity, kni\_proximal\_minimal and VT33935 has been shortened to kni\_pm and  
1054 VT, respectively, in the following graphs. In panels **(C – G)**, (left) split violin plots (and their  
1055 associated box plots) of burst properties for all eight constructs will be plotted with promoter 1 in  
1056 light purple and promoter 2 in purple. The black boxes span the lower to upper quartiles, with the  
1057 white dot within the box indicating the median. Whiskers extend to  $1.5 \times IQR$  (interquartile range)  $\pm$   
1058 the upper and lower quartile, respectively. (right) Bar graphs representing the relative  
1059 contributions of enhancer, promoter, and their interactions to each burst property are plotted as  
1060 described in **(B)**. The double hash marks on the axes indicate that 90% of the data is being shown.  
1061 **(C)** Expression levels are mainly determined by the enhancer and the interaction terms. Some  
1062 enhancers (kni\_-5 and kni\_proximal\_minimal) appear to work well with both promoters; whereas,  
1063 kni\_KD and VT, which are bound by similar TFs, show much higher expression with promoter 2.  
1064 **(D)** Burst frequency is dominated by the enhancer and promoter terms, with promoter 2  
1065 consistently producing higher burst frequencies regardless of enhancer. **(E)** Burst size, which is  
1066 determined by both initiation rate and burst duration, is dominated by the enhancer and interaction  
1067 terms, with interaction terms representing the role of molecular compatibility. As **(F)** burst duration  
1068 is reasonably consistent regardless of enhancer or promoter, differences in burst size are mainly  
1069 dependent on differences in **(G)** PolII initiation rate.  
1070



1071  
1072  
1073  
1074  
1075  
1076

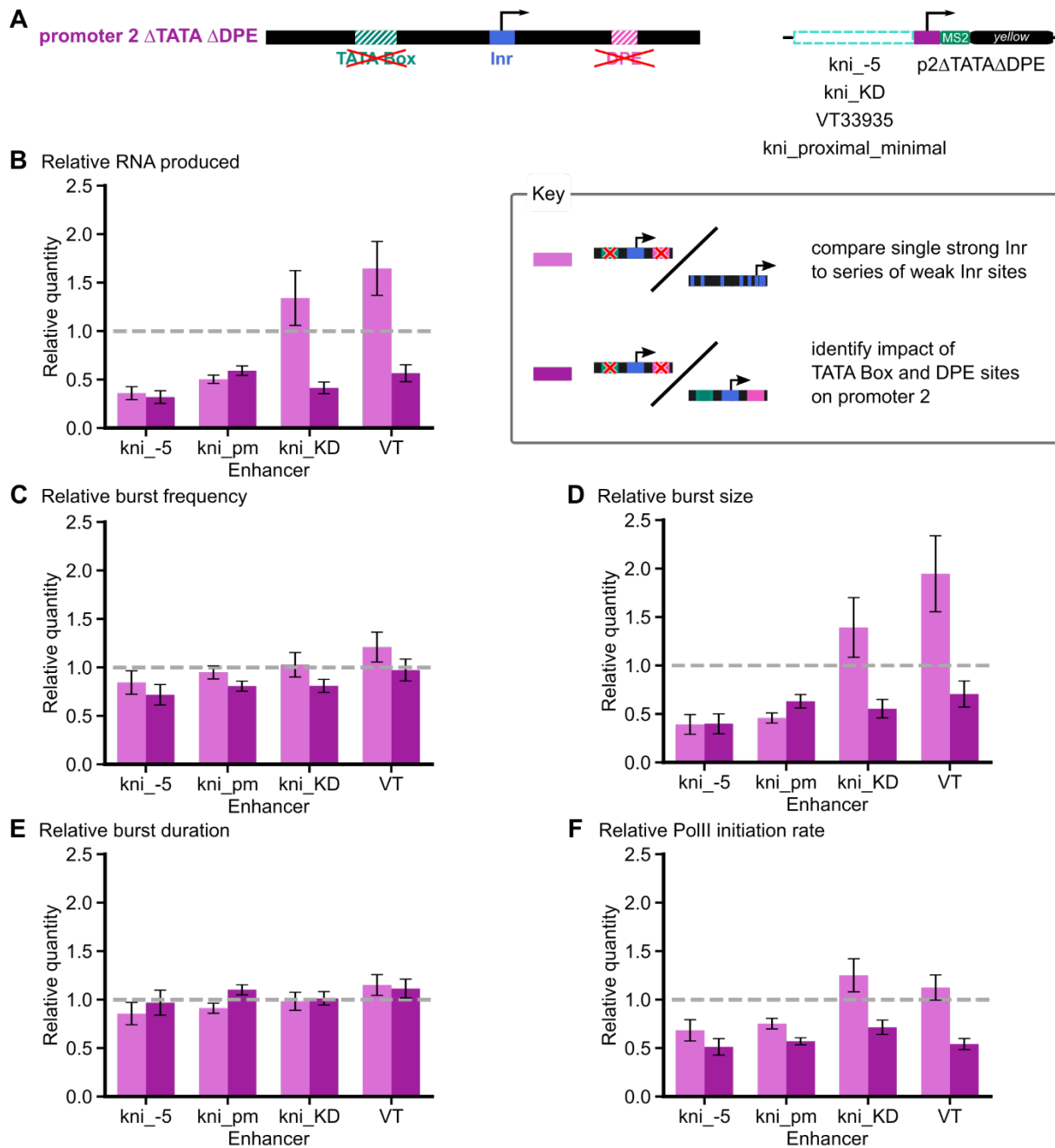
**Figure 5. The synthetic enhancer-promoter constructs are insufficient to capture the behavior of the *knirps* promoters within the endogenous locus.**

**(A)** We cloned the entire *kni* locus into an MS2 reporter construct and measured the expression levels and dynamics of the wildtype (wt) locus reporter, and reporters with either promoter 1 or 2 knocked out ( $\Delta p1$  and  $\Delta p2$ ). To make the  $\Delta p1$  reporter, we replaced promoter 1 with a piece of



1077 lambda phage DNA, due to the large number of Inr motifs. To make the  $\Delta p2$  construct, we  
1078 removed the TATA, Inr, and DPE motifs by making several mutations (see Methods for additional  
1079 details).

1080 In panels **(B – G)**, all burst property data was taken from the anterior-posterior bin of maximum  
1081 expression (22% and 63%) for the anterior band and the posterior stripe, respectively. **(B)** The  
1082 *Drosophila* embryo with the *kni* expression pattern at nuclear cycle 14 is shown; *kni*\_5 drives the  
1083 expression of the anterior, ventral band, while the other three enhancers drive the expression of  
1084 the posterior stripe. The bin of maximum expression is highlighted in light teal. To compare the  
1085 expression produced by the synthetic enhancer-promoter reporters with the locus reporters, we  
1086 plotted bar graphs of the summed total RNA produced at the location of maximum expression in  
1087 the anterior (left) and posterior (right) for six cases—just enhancer-promoter1 reporters (light  
1088 purple), just enhancer-promoter2 reporters (purple), both enhancer-promoter1 and -promoter2  
1089 reporters (dark purple), the wt locus reporter (black), the locus  $\Delta p2$  reporter (light gray), and the  
1090 locus  $\Delta p1$  reporter (dark gray). In panels **(C - F)** violin plots (and their associated box plots) of  
1091 burst properties for all three reporters are plotted with the wt,  $\Delta p1$ , and  $\Delta p2$  reporters in black,  
1092 light gray, and dark gray, respectively. The internal boxes span the lower to upper quartiles, with  
1093 the dot within the box indicating the median. Whiskers extend to  $1.5^*IQR$  (interquartile range)  $\pm$   
1094 the upper and lower quartile, respectively. The double hash marks on the axes indicate that 95%  
1095 of the data is being shown. **(C)** The coefficient of variation is inversely correlated with total RNA  
1096 produced shown in **(B)**. In the anterior, the  $\Delta p2$  reporter, which produces the same total RNA as  
1097 the wt reporter, also produces the same amount of noise. **(D)** In the anterior of the embryo, burst  
1098 frequency of the  $\Delta p2$  reporter is less than the wt reporter even though they produce the same  
1099 expression levels and noise. In the posterior, knocking out promoter 2 has a larger impact on  
1100 burst frequency than knocking out promoter 1. **(E)** In both the anterior and posterior, burst size is  
1101 directly correlated with total RNA produced. Note that in the posterior of the embryo, knocking out  
1102 promoter 2 has a much larger impact on burst size than knocking out promoter 1. Burst size is  
1103 dependent on PolII initiation rate and burst duration. While **(F)** burst duration is reasonably  
1104 consistent regardless of promoter knockout, **(G)** PolII initiation rate is directly correlated with burst  
1105 size. This suggests that differences in burst size are mainly mediated by differences in PolII  
1106 initiation rate.



1107

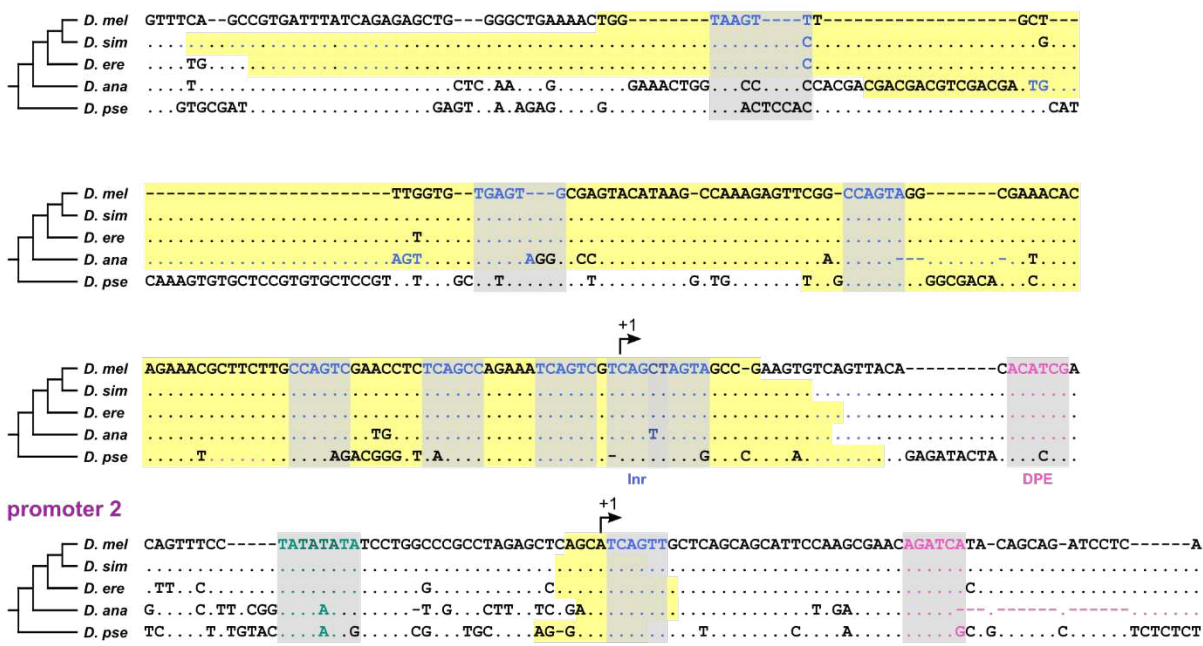
1108

**Figure 6. PolII initiation rate is a key burst property that is tuned by promoter motif.** (A) We made enhancer-promoter reporters containing each of the four enhancers matched with a mutated promoter 2 (p2 $\Delta$ TATA $\Delta$ DPE) in which the TATA Box and DPE motifs have been eliminated by making several mutations (see Methods for details). In panels (B – F), bar graphs of the burst properties produced by p2 $\Delta$ TATA $\Delta$ DPE relative to promoter 1 (in light purple) and to promoter 2 (in purple) are shown. By comparing p2 $\Delta$ TATA $\Delta$ DPE with promoter 1, we can determine whether a single, strong Inr site (mutated promoter 2) can perform similarly to a series of weak Inr sites (promoter 1), and by comparing p2 $\Delta$ TATA $\Delta$ DPE with promoter 2, we can clarify the role of TATA Box and DPE motifs in tuning burst properties. The error bars show the 95% confidence intervals. The gray dashed line at 1 acts as a reference—if there is no difference

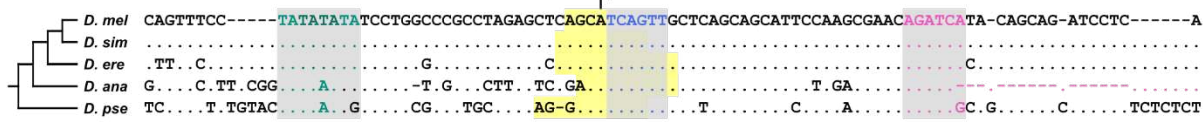
1118 between the burst properties produced by p2ΔTATAΔDPE and either promoter 1 or 2, the bar  
1119 should reach this line. All burst property data was taken from the anterior-posterior bin of  
1120 maximum expression (22% and 63%) for the anterior band and the posterior stripe, respectively.  
1121 Note that for simplicity, kni\_proximal\_minimal and VT33935 have been shortened to kni\_pm and  
1122 VT, respectively, in the following graphs. **(B)** When comparing p2ΔTATAΔDPE with promoter 1,  
1123 we can see that the enhancers fall into two classes—those that drive less expression or more  
1124 expression with a single strong Inr site than with a series of weak Inr sites. The enhancers (kni\_-  
1125 5 and kni\_proximal\_minimal) that drive less expression are the same ones that were similarly  
1126 compatible with both promoters 1 and 2, whereas the enhancers that drive more expression  
1127 (kni\_KD and VT33935) are the ones that strongly preferred promoter 2. When comparing  
1128 p2ΔTATAΔDPE with promoter 2, we see that eliminating TATA Box and DPE motifs reduces  
1129 expression output for all enhancers. **(C)** When comparing p2ΔTATAΔDPE with either promoter 1  
1130 or promoter 2, we see that burst frequency is not substantially affected though, compared to  
1131 promoter 2, there is a moderate decrease upon motif disruption. **(D)** When comparing the burst  
1132 size of p2ΔTATAΔDPE reporters with either that of promoter 1 or promoter 2 reporters, we see  
1133 the same behavior as with total RNA (shown in panel B). This suggests that burst size is the main  
1134 mediator of the increase or decrease in total RNA produced. Burst size is dependent on PolII  
1135 initiation rate and burst duration. As **(E)** burst duration is reasonably consistent regardless of  
1136 promoter, it appears that **(F)** changes in burst size are mainly mediated by tuning PolII initiation  
1137 rate. Together, this suggests that enhancers fall into two classes, based on their response to  
1138 different promoters; however, regardless of class, PolII initiation rate is what underlies differences  
1139 in expression output.

1140  
1141  
1142  
1143

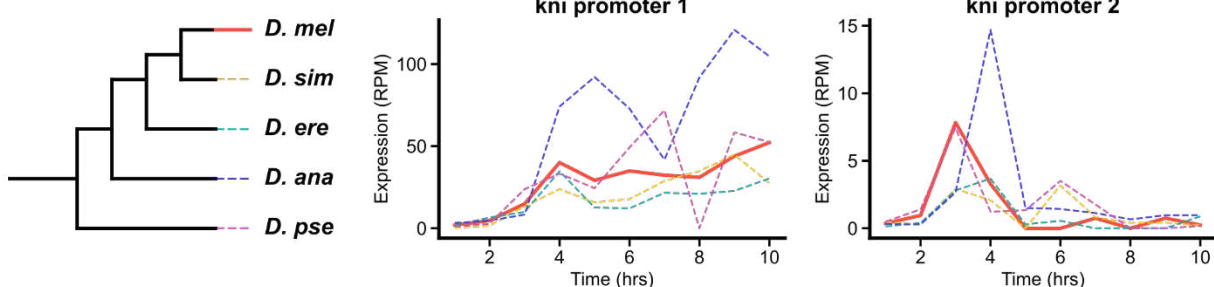
**A promoter 1**



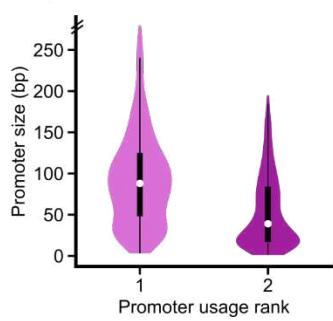
**promoter 2**



**B**



**C All genes**



1144

1145

**Figure S1. The *knirps* promoters show sequence and functional conservation, and this two-promoter structure is prevalent among genes expressed during development.**

1146 (A) Both *kni* promoters are aligned with the orthologous sequences in four other *Drosophila*

1147 species, with dashes (-) representing unaligned sequence and dots (.) indicating matching base

1149 pairs. There is remarkable sequence conservation, with the core promoter motifs preserved

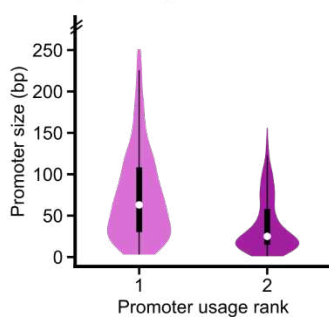
1150 across all five species. The highlighted regions represent transcription start clusters (TSCs),

1151 identified by Batut, et al (P. J. Batut & Gingeras, 2017) as regions of statistically significant

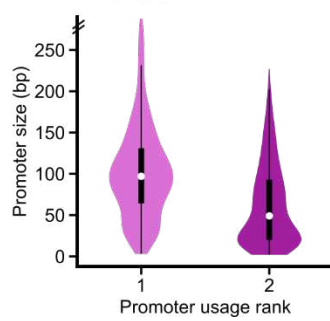
1152 clustering of cDNA 5' ends. (B) *Kni* promoter activity over the first 10 hours of development is

1153 reasonably consistent across five species of *Drosophila*, with promoter 1 generally being used

**D Developmental genes**



**E Housekeeping genes**



1154 more than promoter 2. Specifically, note that both promoters are used in nuclear cycle 14 (2-3  
1155 hours) in all five species. **(C – E)** For developmentally expressed genes with multiple promoters  
1156 that are represented in both the Eukaryotic Promoter Database and the Batut *et al.* RAMPAGE  
1157 data (P. J. Batut & Gingeras, 2017; Dreos, Ambrosini, Cavin Périer, & Bucher, 2013), violin plots  
1158 of the two most used promoters, with the primary promoter (most used) in light purple and the  
1159 secondary promoter (second most used) in dark purple. The black boxes span the lower to upper  
1160 quartiles, with the white dot within the box indicating the median. Whiskers extend to  $1.5^*IQR$   
1161 (interquartile range)  $\pm$  the upper and lower quartile, respectively. The double hash marks on the  
1162 axes indicate that 95% of the data is being shown. **(C)** When the two most used promoters of  
1163 genes expressed in embryogenesis ( $n = 1177$ ) are plotted, the size of primary promoters is  
1164 significantly larger than that of the secondary promoter. **(D)** When limited to promoters of  
1165 developmentally controlled genes – genes whose expression pattern varies considerably as a  
1166 function of developmental time -- ( $n = 387$ ) this trend of larger primary promoters is maintained,  
1167 though on average, these promoters are sharper than those of the whole gene set in panel C. **(E)**  
1168 When limited to promoters of housekeeping genes ( $n = 790$ ), this trend of larger primary than  
1169 secondary promoters is also maintained, though on average, these promoters are still broader  
1170 than those of developmentally controlled genes.  
1171

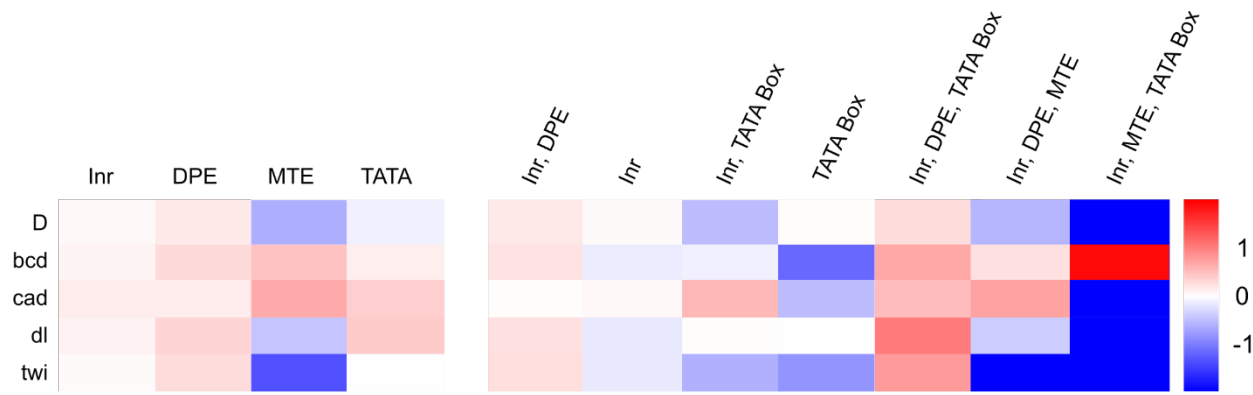


**Figure S2. TFs show preferences for certain core promoter motifs.** To identify patterns of TF-core promoter motif co-occurrence, we calculated the fold enrichment of core promoter elements associated with TF-target genes. The left heatmap shows the log fold-enrichment over background of the frequency of the core promoter motif (columns) for the set of promoters associated with enhancers controlled by the TF (rows). The right heatmap shows the log fold-enrichment over background of the frequency of the motif combination (columns) for the set of promoters associated with enhancers controlled by the TF (rows). For example, this means that column 1 (Inr) in the left heatmap shows enrichment of any promoters that contain Inr regardless of any other promoter motifs they might contain, whereas column 1 (Inr) in the right heatmap shows enrichment of promoters with only Inr and no other core promoter motifs.

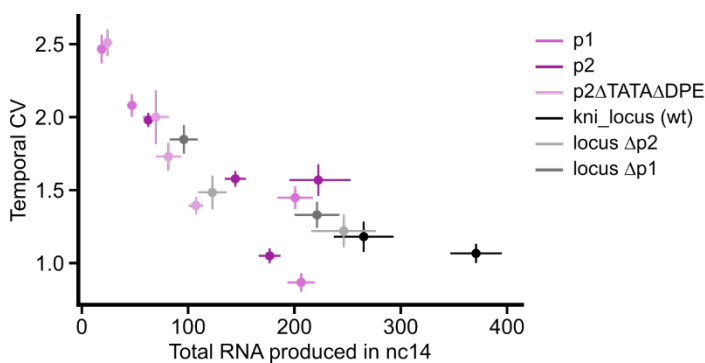
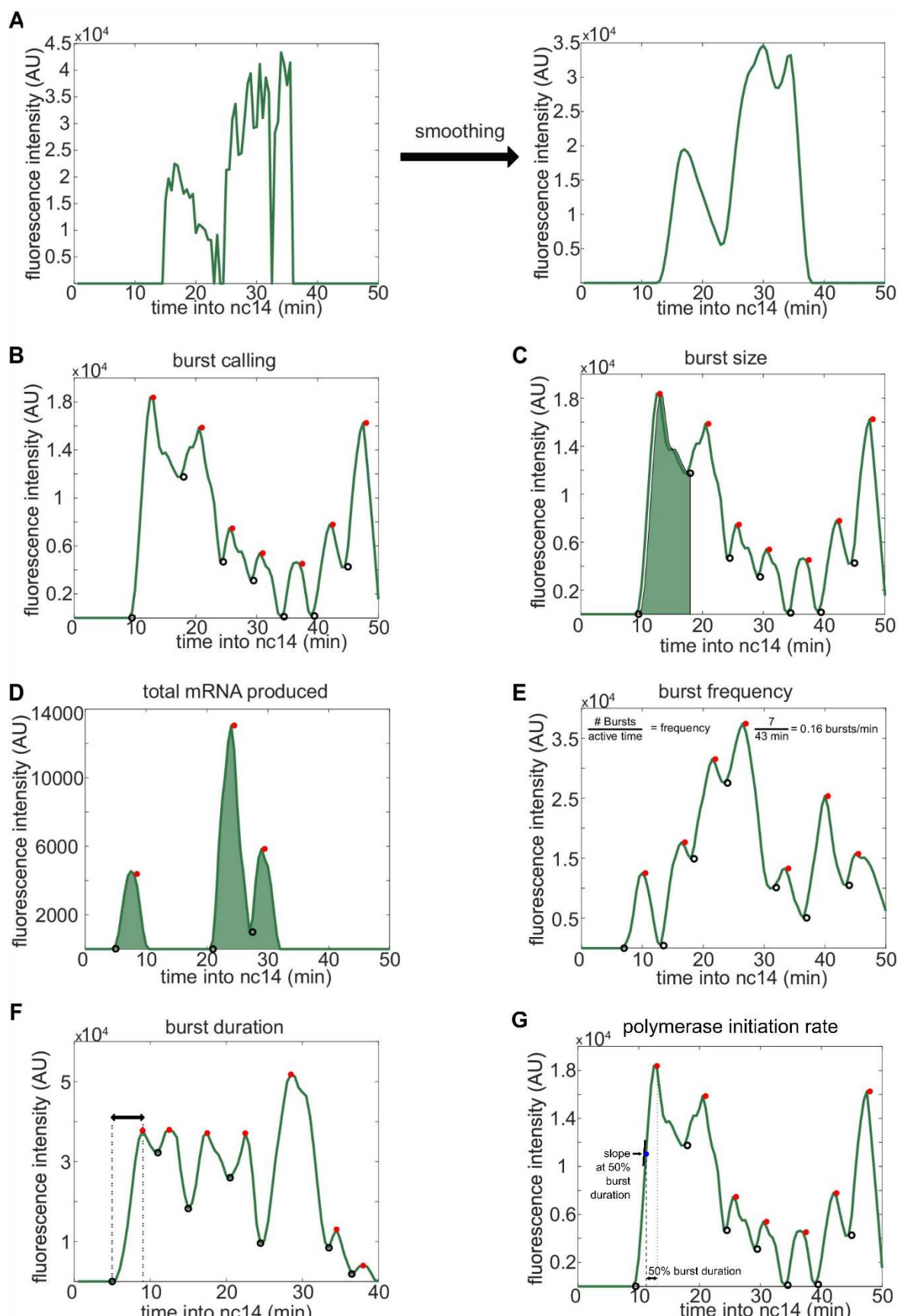
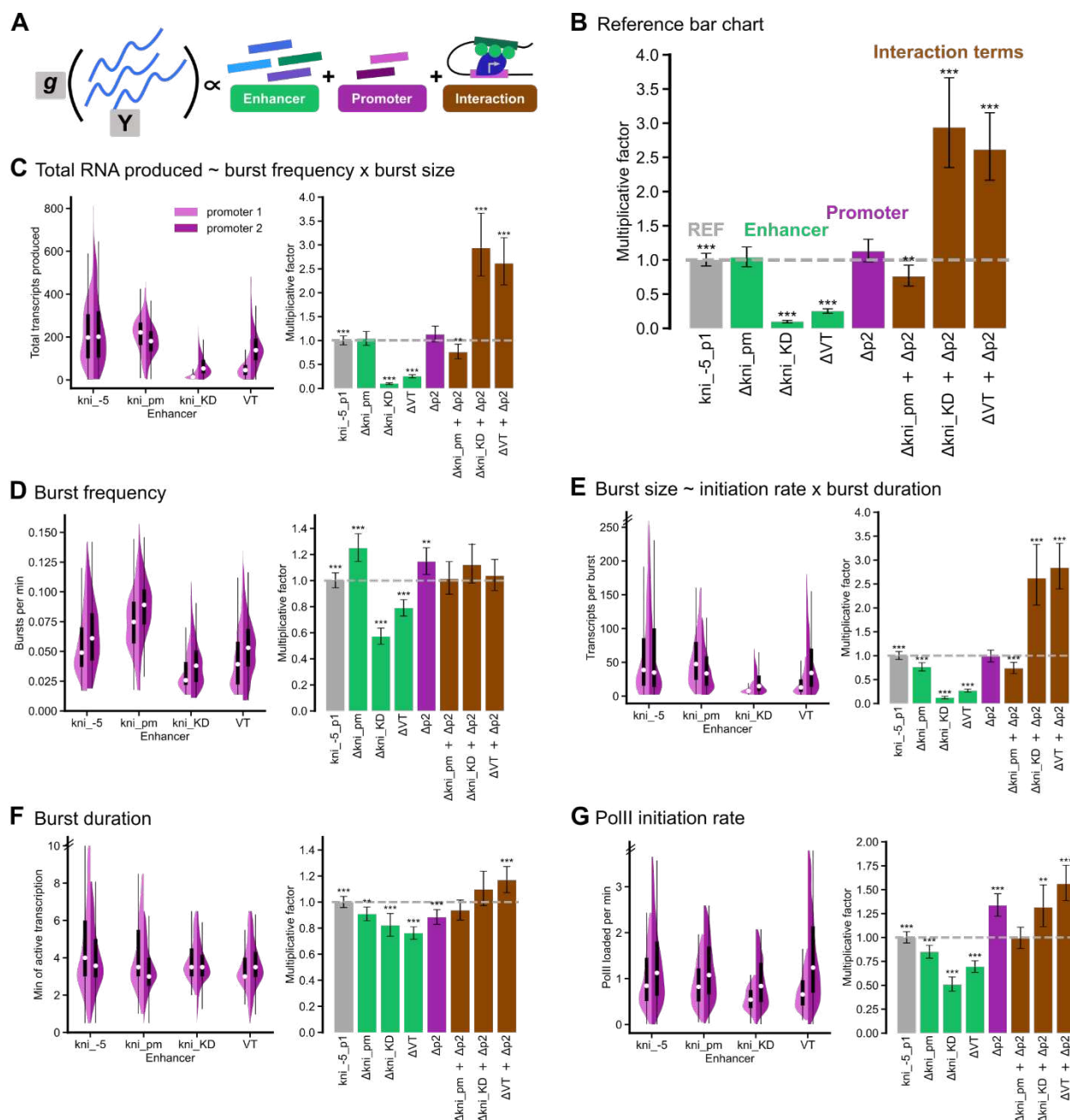


**Figure S3. Noise is inversely correlated with total RNA produced.** To examine the relationship between temporal coefficient of variation (CV) and activity of each construct, we plotted the mean temporal CV against the total RNA produced in nc14 at the anterior-posterior bin of maximum expression (22% and 63%) for the anterior band and the posterior stripe, respectively, with the error bars representing 95% confidence intervals. There is a clear trend of CV decreasing with increased total RNA produced though there are examples where constructs with the same promoter can produce higher noise than others with similar output levels, suggesting that promoters do not solely dictate noise levels.



1198 **Figure S4. Visual inspection of burst calling algorithm.** This figure is adapted from Waymack,  
1199 et al. with one additional panel (**G**) added (Waymack et al., 2020). To quantify the burst properties  
1200 of interest (burst size, burst frequency, burst duration, and polymerase initiation rate), we began  
1201 by smoothing individual fluorescence traces using the LOWESS method with a span of 10%.  
1202 Periods of promoter activity or inactivity were then determined based on the slope of the  
1203 fluorescence trace. **(A)** Example of smoothing transcriptional traces. **(B)** Fluorescence trace of a  
1204 single punctum during nc14. Open black circles indicate time points where the promoter has  
1205 turned “on”, filled red circles indicate time points where the promoter is identified as turning “off”.  
1206 **(C)** Transcriptional trace with the green shaded region under the curve used to calculate the size  
1207 of the first burst. This area of this region is calculated using the trapz function in MATLAB and  
1208 extends from the time point the promoter is called “on” until the next time it is called “on”. Panels  
1209 **(D – F)** show additional representative fluorescence traces of single transcriptional puncta during  
1210 nc14. **(D)** A trace with the entire region under the curved shaded green represents the area used  
1211 to calculate the total amount of mRNA produced. This area is calculated using the trapz function  
1212 in MATLAB extends from the time the promoter is first called “on” until 50 min into nc14 or the  
1213 movie ends, whichever comes first. **(E)** Burst frequency is calculated by dividing the number of  
1214 bursts that occur during nc14 by the length of time from the first time the promoter is called “on”  
1215 until 50 min into nc14 or the movie ends, whichever comes first. **(F)** Burst duration is calculated  
1216 by taking the amount of time between when the promoter is called “on” and it is next called “off”.  
1217 **(G)** Polymerase initiation rate is calculated by taking the slope of the smoothed fluorescence race  
1218 at the midpoint between when the promoter is called “on” and it is next called “off”.  
1219



1220  
1221  
1222  
1223  
1224  
1225  
1226  
1227  
1228  
1229  
1230

**Figure S5. Using canonical link functions gives the same results** Here, we show the results from the generalized linear models (GLMs) when using the log link function instead of the identity link function, which was used in Figure 4.

(A) To parse the effects of the enhancer, the promoter, and their interactions on all burst properties, we built GLMs. Y represents the burst property under study, g is the link function, and the enhancers, promoters, and their interaction terms are the explanatory variables. The coefficients of each of these explanatory variables is representative of that variable's contribution to the total value of the burst property. (B) All burst property data was taken from the anterior-posterior bin of maximum expression (22% and 63%) for the anterior band and the posterior stripe, respectively. We exponentiate the coefficients and the 95% confidence intervals for each

1231 independent variable to invert the log link function and call these quantities the “multiplicative  
1232 factors.” Performing this conversion yields a multiplicative relationship between our response  
1233 variable (the burst property) and our explanatory variables. The reference construct (kni\_-5-p1)  
1234 has been set to 1 such that multiplying the relevant multiplicative factors gives you the value that,  
1235 if multiplied by the reference construct value, will give you the average value of the burst property  
1236 for a particular construct. These factors are plotted as a bar graph; \*  $p < 0.05$ , \*\*  $p < 0.01$ , \*\*\*  $p <$   
1237 0.001. The reference construct is represented in gray, and the effects of enhancer, promoter, and  
1238 their interactions are represented in green, purple, and brown, respectively. Thus, the average  
1239 value of the burst property for a particular construct, e.g. VT-p2, relative to the reference construct  
1240 would be 0.73, which is the product of  $\Delta VT = 0.25$ ,  $\Delta p2 = 1.1$ , and  $\Delta VT + \Delta p2 = 2.6$ . The average  
1241 value of the burst property for VT-p2 would then be  $0.73 \times 205 = 150$ . Note that for simplicity,  
1242 kni\_proximal\_minimal and VT33935 has been shortened to kni\_pm and VT, respectively, in the  
1243 following graphs. In panels **(C – G)**, (left) split violin plots (and their associated box plots) of burst  
1244 properties for all eight constructs will be plotted with promoter 1 in light purple and promoter 2 in  
1245 purple. The black boxes span the lower to upper quartiles, with the white dot within the box  
1246 indicating the median. Whiskers extend to  $1.5 \times \text{IQR}$  (interquartile range)  $\pm$  the upper and lower  
1247 quartile, respectively. (right) Bar graphs representing the relative contributions of enhancer,  
1248 promoter, and their interactions to each burst property are plotted as described in **(B)**. The double  
1249 hash marks on the axes indicate that 90% of the data is being shown. **(C)** Expression levels are  
1250 mainly determined by the enhancer and the interaction terms. Some enhancers (kni\_-5 and  
1251 kni\_proximal\_minimal) appear to work well with both promoters; whereas, kni\_KD and VT, which  
1252 are bound by similar TFs, show much higher expression with promoter 2. **(D)** Burst frequency is  
1253 dominated by the enhancer and promoter terms, with promoter 2 consistently producing higher  
1254 burst frequencies regardless of enhancer. **(E)** Burst size, which is determined by both initiation  
1255 rate and burst duration, is dominated by the enhancer and interaction terms. As **(F)** burst duration  
1256 is reasonably consistent regardless of enhancer or promoter, differences in burst size are mainly  
1257 dependent on differences in **(G)** PolII initiation rate, with this burst property as the main molecular  
1258 knob affected by molecular compatibility.